APPENDIX 1

Principal applications

The following list catalogues some of the principal applications of lock-in amplifiers and phase-sensitive detectors. The compilation was made by the staff at EG & G Brookdeal and covers a wide range of disciplines in applied science and technology. It is inevitable that a number of applications appear under more than one title. To compensate for this, many readers will doubtless find a number of important applications that have been overlooked!

Absorption spectroscopy
A.C. bridges
Antenna Patterns
Astronomical spectroscopy
Atomic absorption
Audio amplifier frequency response
Audiometry
Auger spectroscopy

Biomedical stimuli response measurements
Bode plots

Cochlea microphonics
Common mode rejection measurements
Complex impedance measurements
Contact potential measurements
Crosstalk in cables, amplifiers, etc.
C-*V* plotting
Cube interferometry

De Haas Van Alphen effect
Densitometry
Detectivity compensation
Displacement measurements
Doppler measurements
Dual-beam optical measurements

Eddy-current flaw testing
Edge shift in GaAs
Electrochemistry
Electroluminescence
Emission spectroscopy
E.P.R./e.s.r. spectroscopy

Filter calibration
Fluorescence spectroscopy
Frequency-response measurements
Frequency-shift measurements

Hall effect: single frequency
Hall effect: double frequency

Infra-red (near and far) spectroscopy
Interferometry

Klystron stabilization

Laser research
Line ripple measurement in amplifier power supplies

Magnetic-field measurements
Magnetometry
Magnetoresistance studies
Marx gauging
Mass spectroscopy
Microphone calibration
Microwave reflections, attenuation
Microwave spectroscopy
Moisture content measurement (*C*-*G*)
Molecular-beam spectroscopy

N.M.R. spectroscopy
N.O.R. spectroscopy
Nyquist plots

Operational amplifier gain measurement
Optical derivative measurements

Photometry
Plasma-physics research
Pyrometry

Radiometry
Raman spectroscopy
Ratiometric measurements
Resistance thermometry
R.F. measurements

Second sound
Seismic measurements
Semiconductor research
Source compensation
Spectrophotometry
Strain gauging

Stress-strain measurements

Temperature control
Temperature measurement
Torque measurements

Ultra-violet spectroscopy

Visible spectroscopy

Whistler signal measurements
Work function measurements

Young's modulus

Zeeman effect

Selected topics on signals and noise

A2.1 Introduction

Fig. A2.1 shows the frequency ranges which can be assigned to a number of noise sources of practical importance. As explained in Chapter 2, we usually make a distinction between interference sources of external origin and noise which is inherent in the measurement system. The means to combat external interference sources are many and varied but inevitably involve the use of screening and attention being paid to cable runs. In many cases, susceptibility to mains-frequency pick-up can be reduced by physical re-orientation of circuits and components; factors giving rise to ground loops whereby mains-borne interference is introduced along with the signal are treated in Appendix 6.

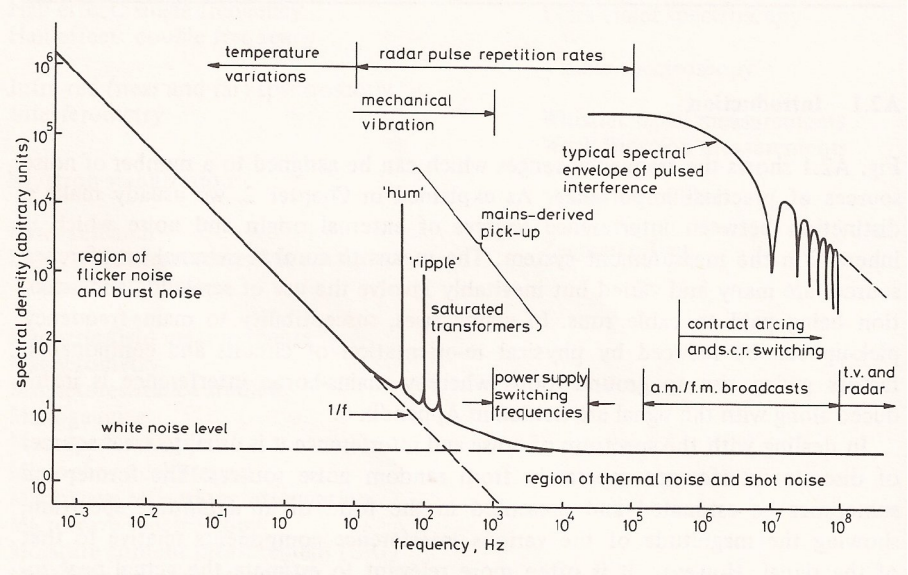

Fig. A2.1 Spectrum of noise and interference

In dealing with the spectrum of noise and interference it is usual to treat sources of discrete interference separately from random noise sources. The former can sometimes be estimated and presented in the form of an *amplitude* spectrum, showing the magnitude of the various interference components relative to that of the signal. However, it is often more relevant to estimate the actual *peak-to-peak* values of the interference components; these components often give rise to saturation in amplifiers, which is most conveniently expressed in peak-to-peak terms.

Of course, the fundamental system noise cannot be treated in terms of an amplitude spectrum. The noise manifests itself as a fluctuating voltage in the output, which is the resultant of components distributed over a wide frequency range. It is characteristic of 'well-behaved' noise sources, however, that these essentially random fluctuations deliver a consistent average power into an external load circuit. In view of this, it is appropriate to express the frequency

distribution of the random noise components in terms of a *power* spectrum or, more exactly, a *power density* spectrum, $P(f)$. $P(f)$ is usually a continuous function of frequency and has dimensions of watts/Hz. By definition of a *density* spectrum the power delivered from a small frequency range Δf centered at a frequency f is simply $P(f)\Delta f$. Therefore, when $P(f)$ is specified, we can calculate the total power in any desired frequency range f_1 to f_2 from the integral

$$P_{\mathrm{TOT}} = \int_{f_1}^{f_2} P(f)\mathrm{d}f$$

This is shown graphically in Fig. A2.2 for a *white noise* spectrum with constant spectral density P_0 and for a more typical spectrum which might be encountered in practice. In both cases the total noise power in the frequency range of interest is given by the area under the spectral density plot.

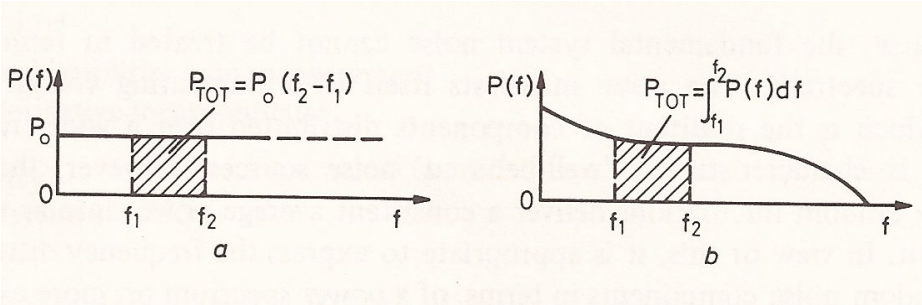

Fig. A2.2 Power density spectra for (a) white noise; (b) typical experimental noise
The total noise power in the frequency range f_1 to f_2 is given by the area of the shaded region in each case

A2.2 Voltage noise and current noise spectra

The integral of a power spectrum is given practical significance when a bandpass filter is used to reject all noise components except for those lying in a selected frequency range. The value of the integral then gives a measure of the noise power which might be measured in the filter output.

In practice, noise power measurements are usually reserved for v.h.f. and other systems operating with well-defined impedance levels. Elsewhere, it is generally more convenient to measure the filter output in terms of its *mean-square* value. Since we are concerned here with electronic systems, the output from the filter will either be a voltage fluctuation or attributable to a current fluctuation: so we express the noise intensity in a given frequency range as a total mean-square voltage or current as appropriate.

This change of emphasis leads us to define mean-square voltage and current noise spectra, $W_{\mathrm{V}}(f)$ and $W_{\mathrm{I}}(f)$, expressed in units V^2/Hz and A^2/Hz respectively. In a given frequency range we measure a voltage signal or a current signal in association with a total mean-square fluctuation:

$$\overline{v^2} = \int_{f_1}^{f_2} W_{\mathrm{V}}(f)\mathrm{d}f$$

or

$$\overline{i^2} = \int_{f_1}^{f_2} W_{\mathrm{I}}(f)\mathrm{d}f$$

A further point remains to be considered. In manufacturers' data sheets, the noise inherent in transducers and amplifiers is commonly given as an *r.m.s.* fluctuation

measured in a specified bandwidth. If a noise voltage has a spectral density expressed in V^2/Hz, then the r.m.s. spectral density must have dimensions V/√Hz. Thus, doubling the measurement bandwidth for a white-noise spectrum doubles the measured intensity while the r.m.s. value increases by only √2.

A2.3 Signal spectra

It is clear that signals have a different status to noise in that a fairly precise description can often be given of their time-domain behaviour. Indeed, as has often been remarked, we must have at least an outline description for a signal before we can embark on the process of signal recovery.

In the restricted view of signal recovery which includes lock-in techniques, the signal is usually an amplitude- or phase-modulated carrier described by one of the general forms:

$$s(t) = A_0 [1 + m(t)] \cos\omega_0 t$$

or

$$s(t) = A_0 \cos [\omega_0 t + m(t)]$$

In each case, the carrier frequency ω_0 is known within fairly close limits and the information or modulation signal, $m(t)$, is to be determined. Just as we have general information about the form of the signal, it is likely that the broad characteristics of $m(t)$ will also be known; the experiment itself will set limits to the maximum amplitude range of $m(t)$ and to its maximum rate of change.

In many instances, the signal is of very simple form and can be separated into sinewave components by the use of trigonometric identities, or expanded as a Fourier series. The frequency composition of the signal and its representation as an amplitude spectrum can then be inferred directly from the time domain description.

Elsewhere, a knowledge of Fourier transforms plays a role in deducing the form of the signal spectrum, but a rigorous approach is not necessarily the most beneficial. In most cases, it is usually sufficient to know: (i) the *location* of the spectrum, (ii) the *width* of the spectrum and (iii) the mean-square value of the signal. Even when the modulation $m(t)$ is only broadly specified, these three points can usually be answered. For example, in the case of amplitude-modulated carrier, we have:

$$s(t) = A_0 [\cos\omega_0 t + m(t)\cos\omega_0 t]$$

We suppose that $m(t)$ is a slowly varying function compared with $\cos\omega_0 t$. If the Fourier transform of $m(t)$ exists, and is given by $M(\mathrm{j}\omega)$, then we can use the narrowband transformation:

$$\Im\{m(t)\cos\omega_0 t\}$$

$$= \tfrac{1}{2}M(\mathrm{j}\omega + \mathrm{j}\omega_0) + \tfrac{1}{2}M(\mathrm{j}\omega - \mathrm{j}\omega)$$

The Fourier transform of the signal is thus

$$S(\mathrm{j}\omega) = \frac{A_0}{2}\delta(\omega-\omega_0) + \frac{A_0}{2}\delta(\omega+\omega_0) + \frac{A_0}{2}M(\mathrm{j}\omega+\mathrm{j}\omega_0) + \frac{A_0}{2}M(\mathrm{j}\omega-\mathrm{j}\omega_0)$$

An example is shown in Fig. A.2.3 with the modulation strictly limited to a bandwidth B_m. A knowledge of this bandwidth is sufficient to estimate the width of the spectrum located about the carrier frequency, although the precise shape of the spectrum may not be known. In this way points (i) and (ii) raised above can be answered. Regarding the mean-square value of the signal we have:

$$\overline{s^2(t)} = \frac{A_0^2}{2}[1 + \overline{m^2(t)}]$$

If the frequency range of the signal can be estimated together with its mean-square value we can avoid the need for a formal definition of intensity spectra for periodic and other 'deterministic' signals. Also, we see, that provided $|m(t)| < 1$, we can estimate the signal intensity to within a factor of 2 even when $m(t)$ itself might not be precisely specified. If this seems inadequate in the light of the conventional approach to modulation systems it is no worse than the degree of approximation used in estimating the level of the background noise!

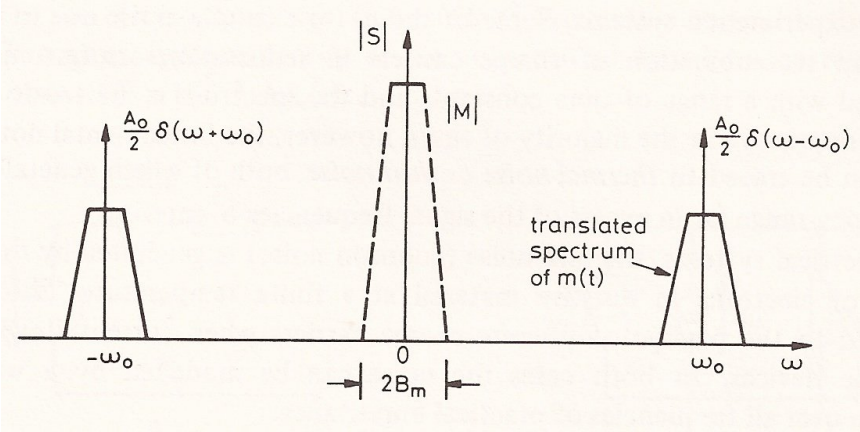

Fig. A2.3 Spectrum of an amplitude-modulated carrier

In the case of phase modulation: when $|m(t)| << 1$, corresponding to low-index modulation, the signal can be expressed as:

$$s(t) = A_0 [\cos\omega_0 t \cos m(t) - \sin\omega_0 t \sin m(t)]$$

$$\cong A_0 [\cos\omega_0 t - m(t)\sin\omega_0 t]$$

The *amplitude* spectrum and the effective bandwidth of $s(t)$ is thus the same as for amplitude modulation by the same information signal $m(t)$. Note, however, that the phase relationships are different in the two cases.

At the other extreme, when the index of modulation is large, Carson's rule can be used to estimate the 'spread' of the spectrum from its centre frequency. This gives an estimate of the signal bandwidth:

$$B_s = 2(|m(t)|_{max} + 1)B_m$$

where B_m is the bandwidth of the modulation or information signal.

When calculating the mean-square value of phase modulated signals, we find that the phase terms make no contribution to the final result. This is simply

$$\overline{s^2(t)} = A_0^2/2$$

In general we might expect that the signal carries *both* amplitude and phase modulation. While this is a possibility we should also note that, in the vast majority of cases, the modulations can be very slowly varying functions, often limited to a bandwidth of a few hertz. Thus, very often, the signals of interest are extremely narrowband, occupying a *relative* bandwidth of no more than a few per cent.

A2.4 Thermal noise and shot noise

There are a number of well defined mechanisms which give rise to broadband* noise in experimental systems. Some of these, for example, noise due to the generation and recombination of charge carriers in semiconductors (g.r. noise), are associated with a range of time constants and the spectrum is limited to an upper cut-off frequency. In the majority of cases, however, the fundamental noise mechanisms can be traced to *thermal noise* or *shot noise*, both of which generally occupy a frequency range far in excess of the signal frequencies of interest.

In electrical systems, thermal noise (Johnson noise) is generated by the random motion of electrons in resistive material at a finite temperature. Shot noise is attributed to the passage of discrete charge carriers when current flows through electronic devices. In both cases the noise can be modelled by a white-noise spectrum over all frequencies of practical importance.

First of all, regarding thermal noise: this is a fundamental source of fluctuation in all physical systems in a state of thermodynamic equilibrium. We can be sure, therefore, that it will be found in all linear, passive devices, irrespective of their form. It is often the case that such devices – and for that matter entire experimental systems – can be reduced to a simple description in terms of an equivalent *electrical analogue* circuit. The most common is either the Thévenin or the Norton form shown in Fig. A2.4.

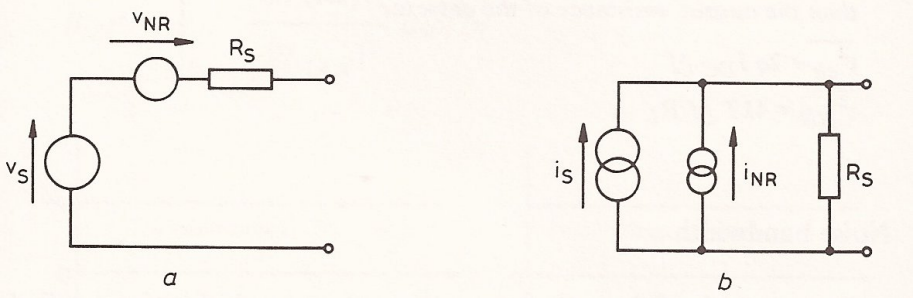

Fig. A2.4 (a) Thévenin and (b) Norton source equivalent circuits including resistance noise generators

The equivalent source resistor is defined in terms of the physical characteristics of the linear device and the thermal noise associated with the source resistance is included in the form of a voltage or current noise generator. When R_s is specified and the temperature is known we can immediately obtain the spectral density functions of these noise generators:

$$W_v(f) = 4\,kTR_s \text{ V}^2/\text{Hz}$$

$$W_I(f) = 4\,kT/R_s \text{ A}^2/\text{Hz}$$

Here, k is Boltzmann's constant (1.38×10^{-23} joules/K), R_s is the equivalent source resistance in ohms and T is the absolute temperature.

In calculations involving resistive sources at laboratory temperature it is convenient to remember that a resistor of x kilohm is associated with a random voltage generator of $4\sqrt{x}$ nanovolts/$\sqrt{}$Hz or a random current generator of $4\sqrt{x}$ picoamperes/$\sqrt{}$Hz.

* 'Broadband' noise is recognised by its having a spectrum that is generally free from local 'peaks' and extends to zero frequency.

Shot noise, unlike thermal noise, is always associated with current flow. The random passage of charge carriers in vacuum tubes and semiconductors gives rise to a fluctuation which depends on the average current. The spectrum is that of white noise which extends over a wide frequency range limited only by transit-time effects in the electronic device. We have

$$W_I(f) = 2qI_0 \ \text{A}^2/\text{Hz}$$

where q is the electronic charge (1.6×10^{-19} coulombs) and I_0 is the average current. The r.m.s. spectral density of the noise caused by a 1 nA current flow is therefore about 1.8×10^{-14} A/√Hz.

Shot noise will be present in all semiconductor devices operating with finite bias current, and is usually the dominant source of broadband noise in optical detectors. Here, a periodic current variation due to a 'chopped' light beam must often be measured against a more or less steady bias current which flows in response to a much greater 'background' illumination due to light leakage or sample fluorescence. Many such detectors conform closely to an ideal current source, and the output can be measured by connecting the detector to an external load resistor R_L. Fig. A2.5 gives the noise equivalent circuit of this arrangement, which shows that the signal current i_s appears in competition with the shot noise of the bias current I_{DC} and the thermal noise of the load resistor. To ensure that the signal-to-noise ratio inherent in the detector is not degraded further by the thermal noise in R_L we investigate the condition:

$$2qI_{DC} \geq 4\,kT/R_L$$

which gives

$$R_L \geq 2kT/(qI_{DC})$$

The quantity $2kT/q$ is approximately equal to 50 mV at laboratory temperatures. Thus, for a bias current of 1 mA, the source will be dominated by shot noise provided that R_L is in excess of 50 Ω. In fact, the usual tendency is to choose very large values of R_L to increase the output voltage due to the signal current. In this case, the shot-noise contribution is usually the dominant one even at low bias currents. This topic is discussed further in Appendix 5 in relation to amplifier selection and the use of current amplifiers.

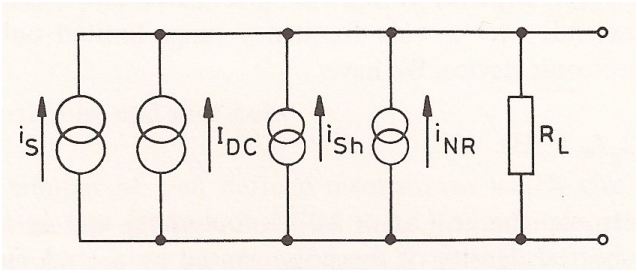

Fig. A2.5 **Noise equivalent circuit for a detector terminated in a resistor R_L. R_L is much less than the output resistance of the detector**

$\overline{i_{sh}^2} = 2q\,I_{DC}\Delta f; \quad \overline{i_{NR}^2} = 4kT\Delta f / R_L$

A2.5 Noise bandwidth

The overall bandwidth of the noise appearing with a signal of interest will always be limited to some finite value, if only because of the effect of stray reactance. More usually, however, the bandwidth is fixed at a well defined value owing to the low-pass filter effect of the transducer and output amplifier.

When the noise inherent in the experimental process is broadband in nature, the combined frequency response of the transducer/amplifier combination is often responsible for the spectral characteristics of the noise observed in the final measurement. For example, suppose the experimental noise has constant spectral density W_N over a wide frequency range, and that we can identify a frequency-response function, $H(j\omega)$, with comparatively narrow bandwidth. The spectrum of the 'output' noise can then be approximated by

$$W(f) = W_N |H(j\omega)|^2, \quad \omega = 2\pi f$$

Conversely, an observed noise spectrum can often be modelled by assuming that it originates from the passage of broadband white-noise through a filter with appropriate frequency-response characteristics. 'Broadband' spectra and 'narrowband' spectra such as those shown in Fig. A2.6 are examples where this approach is often successful.

In order to calculate the total fluctuation due to the noise we integrate its spectrum over all frequencies to obtain the mean-square value:

$$N_0 = W_N \int_0^\infty |H(j\omega)|^2 d\omega / 2\pi$$

Since the integral depends only on the filter transfer function we can simplify all subsequent discussions by defining the *noise equivalent bandwidth* of the filter. This gives the bandwidth of the rectangular filter shown in fig. A2.6 which transmits the same fluctuation as the actual filter of interest.

The noise output of the noise-equivalent rectangular filter with bandwidth B_N is

$$N_0 = W_N |H_{MAX}|^2 B_N$$

hence, equating this with the integrated noise in the filter characteristic $H(j\omega)$, we obtain the filter noise-equivalent bandwidth in terms of the integral:

$$B_N = \int_0^\infty \frac{|H(j\omega)|^2}{|H_{MAX}|^2} d\omega / 2\pi$$

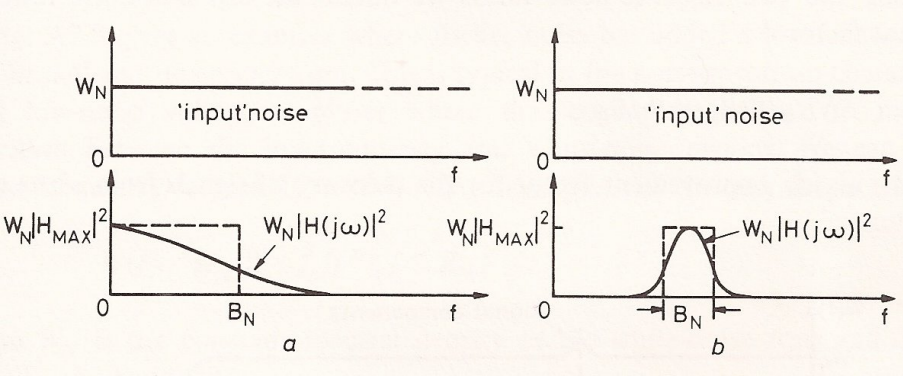

Fig. A2.6 (a) Broadband and (b) narrowband noise spectra obtained by filtering white noise. B_N denotes the noise equivalent bandwidth

The noise-equivalent bandwidth (or, simply, noise bandwidth) of a practical filter is somewhat greater than its 3 dB bandwidth, but becomes closer for filters of higher order. This reflects the sharper cut-off of high-order filters, which approximate more closely to filters with 'ideal' cut-off characteristics.

In principle, therefore, the output fluctuation of any filter in response to a white-noise input can be calculated once the maximum gain of the filter and its noise

bandwidth are known. The latter is usually obtained from a catalogue of noise bandwidths such as that given in Appendix 4.

Finally, it should be noted that noise bandwidth is conventionally expressed in *hertz* and not radians/second.

A2.6 Signal-to-noise-ratio improvement by filtering

We envisage the situation shown in Fig. A2.7, where a signal, $s(t)$, appears against a background of white noise having noise bandwidth B_I and spectral density W_N.

The signal-to-noise ratio, measured on a mean-square basis, is simply

$$SNR_I = \frac{\overline{s^2(t)}}{W_N B_I}$$

A signal-conditioning filter is now used to attenuate all noise components except those lying within the frequency band occupied by the signal. The filter bandwidth is sufficiently wide to transmit the signal without distortion, but significantly smaller than the 'input' noise bandwidth B_I. In this case, the signal-to-noise ratio at the filter output is given to a good approximation by

$$SNR_0 = \frac{\overline{s^2(t)}}{W_N B_0}$$

where B_0 is the noise bandwidth of the filter. Note that the gain modulus of the filter, $|H_{MAX}|$, does not appear in the expression for signal-to-noise ratio.

Dividing the two signal-to-noise ratios we obtain the signal-to-noise ratio improvement factor

$$SNR_0/SNR_I = B_I/B_0$$

This is the classic improvement factor for the recovery of signals from white noise by filtering.

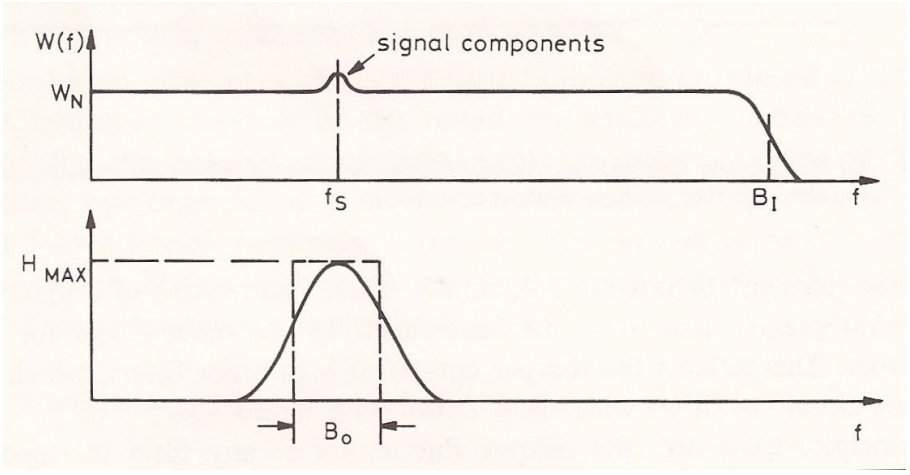

Fig. A2.7 Spectrum of signal and noise shown with the transmission characteristics of a noise reduction filter

A2.7 Low-frequency noise

'Practical' noise spectra almost invariably display a steady rise in spectral density as lower and lower frequencies are taken into account. This is the so-called *flicker-noise* region where the spectral density follows a law

$$W(f) = W_0/f^x$$

Here, W_0 is a constant and x takes values, typically, in the range 0.8 to 1.4. The term '1/*f* noise' is also used to describe spectra of this general type.

Flicker-noise is associated with a wide range of physical processes. Although its origins are obscure, its spectral characteristics are usually well-defined for a given experimental set-up.

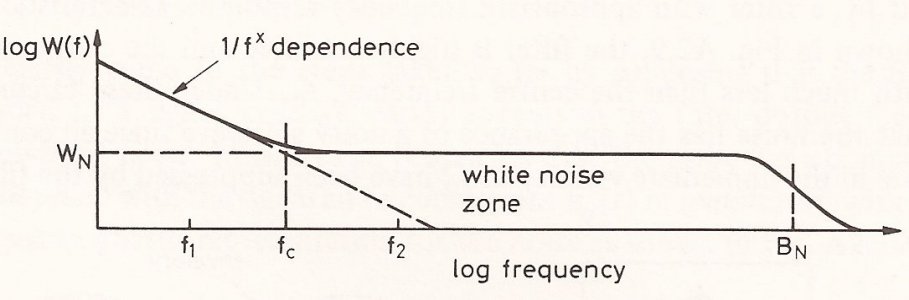

Fig. A2.8 Spectral model for broadband noise with a low-frequency noise component

Fig. A2.8 gives an example where flicker noise has added a low-frequency 'tail' to a broadband noise spectrum. This is typical of the noise-spectrum characteristics of a low-noise voltage amplifier where the 'corner frequency', f_c, marks the transition between the low-frequency and white-noise regions. We can use the corner frequency to provide the following description of the overall spectrum:

$$W(f) = W_N\,[1 + f_c/f^x], \quad f < B_N$$

where W_N is the constant spectral density in the white-noise zone and B_N is the overall noise bandwidth.

The widespread incidence of flicker-noise accounts for the equally widespread use of a.c. excitation in experimental work, the object being to bring the signal of interest into the spectral region above the corner frequency. If a clear separation is not achieved, then it may sometimes be necessary to calculate the total fluctuation from the frequency interval f_1 to f_2 shown in Fig. A2.8 which includes the corner frequency. For the purpose of calculation it is usual to assume that $x = 1$. To do otherwise implies that the spectrum of low-frequency noise has been characterised very carefully.

Our spectral model gives a total mean-square fluctuation:

$$\int_{f_1}^{f_2} W_N\,[1 + f_c/f]\,df = W_N\,(f_1 - f_2) + W_N\,f_c\,\mathrm{1n}\,(f_2/f_1)$$

We thus find that the white-noise component gives rise to a mean-square fluctuation proportional to the measurement bandwidth, $(f_2 - f_1)$, while the flicker-noise contribution depends on the frequency *ratio*. We conclude from this that the flicker-noise fluctuation measured per octave or per decade is constant over all frequencies.

A2.8 More about narrowband noise

The term 'narrowband noise' is generally used to describe noise that has zero spectral density in the vicinity of $f = 0$. It was remarked in Section A2.5 that narrowband noise can often be modelled by supposing that white noise has been transmitted by a filter with appropriate frequency-response characteristics. In the example shown in Fig. A2.9, the filter is highly selective and the output noise has a bandwidth much less than the centre frequency, f_0. Under these circumstances we find that the noise has the appearance of a noisy sinewave since all components except those in the immediate vicinity of f_0 have been suppressed by the filter.

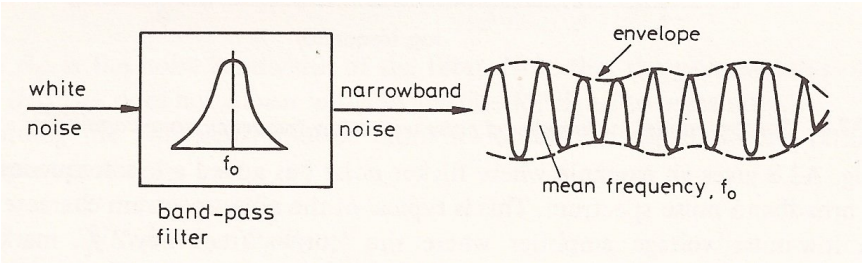

Fig. A2.9 Generation of narrowband noise

We shall find that the structure of narrowband noise lends itself to a time-domain description which proves to be very useful when considering the response of synchronous detectors to noise inputs. To provide a time-domain model we suppose that we start with a 'clean' sinewave at frequency f_0 and then impose random variations on its instantaneous amplitude and phase. The result is a voltage:

$$n(t) = R(t) \cos [\omega_0 t + \phi(t)]$$

$R(t)$ and $\phi(t)$ are random modulations that vary very slowly in comparison with $\cos\omega_0 t$. $\phi(t)$ is a simple phase modulation while Fig. A2.9 shows that we can interpret $R(t)$ as the *envelope*[*] of the noise. Because $R(t)$ is a relatively slow variation, we find that there is no dramatic change in the envelope over several cycles at frequency f_0.

We now expand $n(t)$ into its constituent components to obtain:

$$n(t) = R(t) \cos \phi(t) \cos\omega_0 t - R(t) \sin \phi(t) \sin\omega_0 t$$

and then define:

$$n_i(t) = R(t) \cos \phi(t)$$

$$n_q(t) = R(t) \sin \phi(t)$$

Thus:

$$n(t) = n_i(t) \cos\omega_0 t - n_q(t) \sin\omega_0 t$$

where

$$[n_i^2 (t) + n_q^2(t)]^{1/2} = R(t)$$

and

$$n_q(t)/n_i(t) = \tan\phi(t)$$

[*] An ideal rectifier, incorporating an output low-pass filter, would deliver an output voltage which varied in response to the envelope function, $R(t)$.

We can clarify some of the steps taken so far by supposing that the filter is precisely tuned to a signal, $\cos\omega_0 t$, which appears in the filter output together with the narrowband noise. In this case, it appears that the noise has a component $n_i(t)$ that lies *in-phase* with the signal and a component $n_q(t)$ in *quadrature* with the signal. This suggest a phasor representation for the noise as shown in Fig. A2.10.

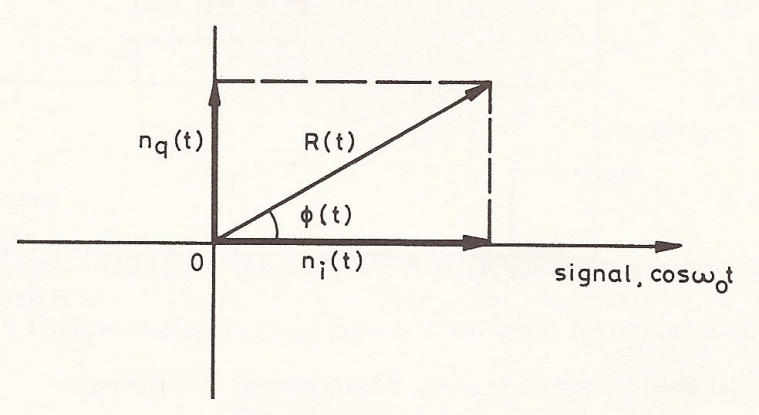

Fig. A2.10 Phasor representation of narrowband noise

Relationships between $n(t)$, $n_i(t)$ and $n_q(t)$ and their spectra are derived in most books on communication theory; for example, Taub and Schilling[1], and Haykin[2], but – for our purposes – it will be sufficient to note the following properties:

(i) *Mean value:* We are, dealing with noise at the output of a bandpass filter which implies that $n(t)$, and hence $n_i(t)$ and $n_q(t)$, have zero mean value, that is:

$$\overline{n(t)} = \overline{n_i(t)} = \overline{n_q(t)} = 0$$

(ii) *Mean-square value:* The phasor diagram shown in Fig. A2.10 is a 'snapshot' taken at a particular instant. The fact that n_i and n_q have zero mean values implies that the noise phasor spends an equal amount of time – on average – in all four quadrants. This symmetry suggests that n_i and n_q have equal mean square values and it can be shown that this is indeed the case:

$$\overline{n_i^2(t)} = \overline{n_q^2(t)}$$

In general, the noise processes $n_i(t)$ and $n_q(t)$ are uncorrelated. Hence, the total mean-square fluctuation of the narrowband noise, $n(t)$, is:

$$\overline{n^2(t)} = \overline{n_i^2(t)\cos^2\omega_0 t} + \overline{n_q^2(t)\sin^2\omega_0 t} = \tfrac{1}{2}\overline{n_i^2(t)} + \tfrac{1}{2}\overline{n_q^2(t)}$$

We thus obtain:

$$\overline{n^2(t)} = \overline{n_i^2(t)} = \overline{n_q^2(t)}$$

(iii) *Spectral density of* $n_i(t)$ and $n_q(t)$: If we denote the spectrum of the narrowband noise by $W_n(f)$, then the spectra of $n_i(t)$ and $n_q(t)$ are identical, obtained through the transformation[1,2]:

$$W_i(f) = W_q(f) = W_n(f - f_0) + W_n(f + f_0)$$

where f_0 is the 'centre frequency' of the narrowband noise process.

$W_i(f)$ and $W_q(f)$ generally have the form of *low-pass* spectra. In the special case where $W_n(f)$ is symmetrical about $f = f_0$, we obtain:

$$W_i(f) = W_q(f) = 2W_n\,(f + f_0)$$

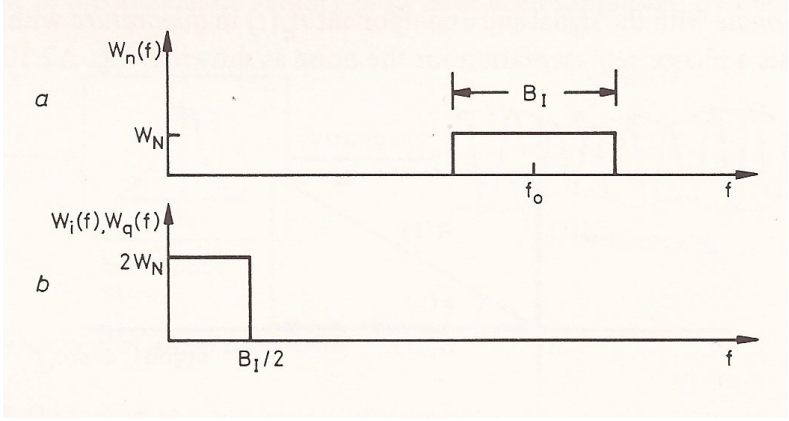

Fig. A2.11 (a) Band-limited white noise; (b) spectrum of $n_I(t)$ and $n_q(t)$

For example, suppose the narrowband noise has the form of band-limited white noise as shown in Fig. A2.11. We have:

$$W_n(f) = \begin{cases} = W_N, & f_0 - B_I/2 \le f \le f_0 + B_I/2 \\ = 0, & \text{elsewhere} \end{cases}$$

In this case, $W_i(f)$ and $W_q(f)$ take the form:

$$W_i(f) = W_q(f) \begin{cases} = 2W_N, & f \le B_I/2 \\ = 0, & \text{elsewhere} \end{cases}$$

Integrating $W_i(f)$, $W_q(f)$ and $W_n(f)$ over all frequencies we confirm the results given earlier, namely:

$$\overline{n_i^2(t)} = \overline{n_q^2(t)} = \overline{n^2(t)}$$

where, in this case:

$$\overline{n^2(t)} = W_N B_I$$

A2.9 References

1 TAUB, H., and SCHILLING, D.L. (1971): Principles of communication systems' (New York, McGraw Hill)

2 HAYKIN, S. (1978): 'Communications systems' (New York, John Wiley & Sons)

Synchronous detection and noise

A3.1 Signal-to-noise-ratio improvement

Let us consider the response of a synchronous detector to an amplitude-modulated signal perturbed by random noise, giving an input of the form:

$$v_{\text{in}}(t) = m(t)\cos\omega_0 t + n(t)$$

We have seen that the operation of synchronous detectors does not necessarily depend on the elimination of unwanted noise components by filtering in advance of detection. However, it was shown in Appendix 2 that the structure of narrow-band noise is particularly convenient when it comes to performing calculations in the time domain. We shall therefore assume that the input noise is band-limited as shown in Fig. A3.1 with a bandwidth B_{I} much greater than the signal bandwidth $2B_{\text{M}}$.

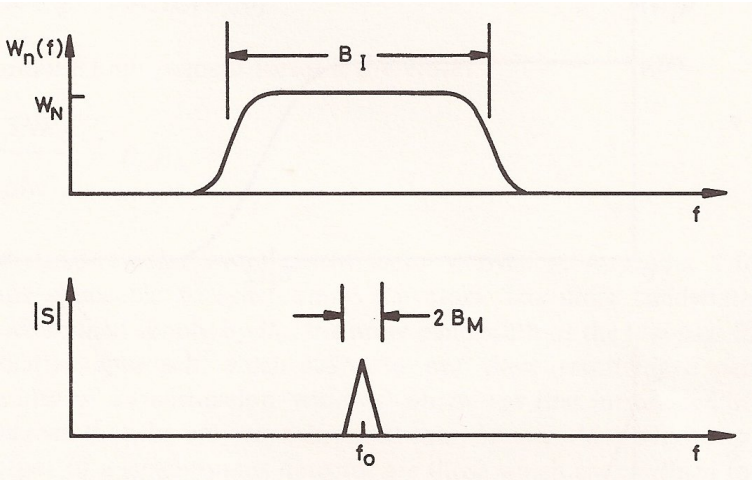

Fig. A3.1 Spectra of: (a) input noise and (b) amplitude-modulated signal

If we further assume that the noise spectrum is centered on the signal frequency, we can use the results of Appendix A2.8 and write:

$$n(t) = n_{\text{i}}(t)\cos\omega_0 t - n_{\text{q}}(t)\sin\omega_0 t$$

The input voltage to the synchronous detector now has the form:

$$v_{\text{in}}(t) = \left[m(t) + n_{\text{i}}(t)\right]\cos\omega_0 t - n_{\text{q}}(t)\sin\omega_0 t$$

Following the arguments developed in Appendix A2.8, we identify $n_{\text{i}}(t)$ and $n_{\text{q}}(t)$ as the components of the noise lying, respectively, in phase and in quadrature with the signal.

A reference voltage, synchronous with the signal of interest, is now introduced at the synchronous detector and the phase is adjusted to bring signal and reference in phase. The reference voltage is:

$$v_R(t) = \sqrt{2} V_R \cos \omega_0 t$$

giving multiplication products:

$$v_{in}(t) v_R(t) = \frac{V_R}{\sqrt{2}} \left[m(t) + n_i(t) \right] \left[1 + \cos 2\omega_0 t \right] - \frac{V_R}{\sqrt{2}} n_q(t) \sin 2\omega_0 t$$

At this stage we shall assume that the output low-pass filter is used only to eliminate components centered on frequency $2\omega_0$ without modifying the low-frequency output of the multiplier. We obtain an output voltage:

$$v_0(t) = \frac{V_R}{\sqrt{2}} \left[m(t) + n_i(t) \right]$$

giving an output signal-to-noise ratio:

$$SNR_0 = \overline{m^2(t)} / \overline{n_i^2(t)}$$

This important result shows that the output signal-to-noise ratio is given in terms of the noise components that lie *in-phase* with reference voltage. We thus conclude that the *quadrature* noise components $n_q(t)$ are rejected at the point of detection and so make no contribution to the low-frequency output.

The input signal-to-noise ratio is:

$$SNR_I = \overline{\left[m^2(t) \cos^2 \omega_0 t \right]} / \overline{n^2(t)} = \tfrac{1}{2} \overline{m^2(t)} / \overline{n^2(t)}$$

From Section A2.8 we have:

$$\overline{n_i^2(t)} = \overline{n^2(t)} = W_N B_I$$

Hence:

$$\frac{SNR_0}{SNR_I} = 2$$

A signal-to-noise improvement factor of 2 is thus inherent in the operation of the synchronous detector.

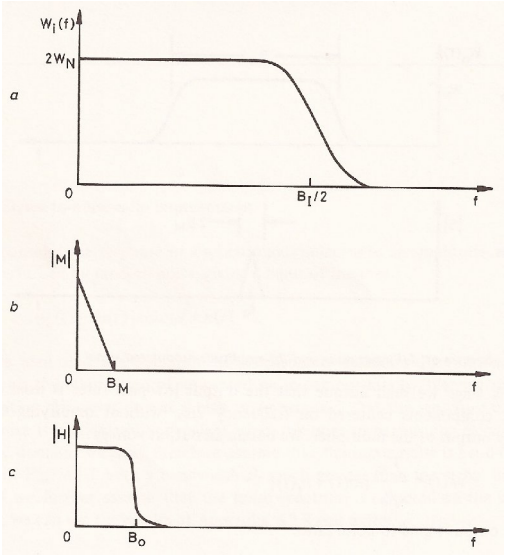

Fig. A3.2 **(a), (b) Spectra of output noise and recovered modulation signal in a synchronous detector; (c) frequency response of noise-reduction filter in final output**

The spectra of the recovered modulation signal and the output noise are shown in Fig. A3.2 for the case where $V_R = \sqrt{2}$. We now suppose that the bandwidth of the low-pass filter is greatly reduced in order to eliminate noise components from the final output. The output noise bandwidth is accordingly set to a value B_0 as indicated in Fig. A3.2 where B_0 is sufficiently wide to transmit the recovered modulation signal without distortion.

When $B_0 << B_I$ we can approximate the mean-square value of the noise following the low-pass filter by:

$$N_0 = 2W_N B_0$$

and so obtain the output signal-to-noise ratio:

$$SNR_0 = \frac{\overline{m^2(t)}}{2W_N B_0}$$

compared with the input signal-to-noise ratio:

$$SNR_I = \frac{\overline{m^2(t)}}{2W_N B_I}$$

The signal-to-noise improvement factor is therefore:

$$\frac{SNR_0}{SNR_I} = B_I / B_0$$

The "classic" signal-to-noise improvement factor derived in Appendix 2 for linear filters is thus applicable to synchronous detectors. The noise bandwidth of the detector is determined simply by B_0, the noise bandwidth of the low-pass filter.

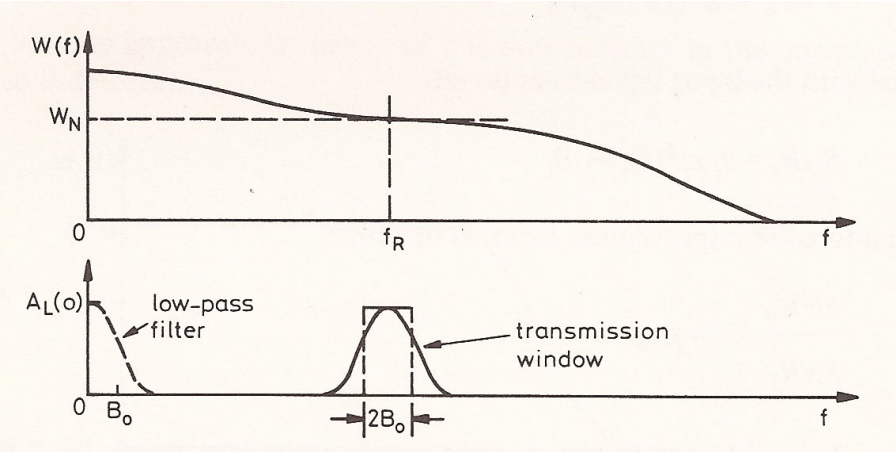

Fig. A3.3 Synchronous detector with arbitrary input noise spectrum

An alternative approach which helps to put these results into perspective involves the idea of a transmission "window" which was first introduced in Section 2.4. We have seen that the only asynchronous components which survive to perturb the final output of a synchronous detector are those which are confined to a transmission window centred on the reference frequency, having a noise bandwidth equal to *twice* the noise bandwidth of the low-pass filter. Using the spectral model shown in Fig. A3.3 for an arbitrary noise spectrum, the mean-square fluctuation associated with the components within the transmission windows is, approximately:

$$N_0 \approx 2B_0 W_N$$

However, from the results given above, it is evident that the synchronous detector responds only to the components of the noise that lie *in-phase* with the reference. Of the total mean-square fluctuation appearing within the transmission window we can ascribe one half to noise components lying in phase with the reference and one half to noise components in quadrature with the reference. If we now suppose that a synchronous detector has a full-scale sensitivity S_F and a full-scale output V_F, the noise appearing in the final output will have a mean-square value:

$$\overline{v_N^2} = \tfrac{1}{2}\left(V_F / S_F\right)^2 N_0 = \left(V_F / S_F\right)^2 B_0 W_N$$

The factor $1/2$ accounts for the loss of the quadrature noise components at the point of detection. Although the synchronous detector transmission window has a noise bandwidth $2B_0$, the rejection of the quadrature noise components results in an *effective* noise bandwidth of B_0.

Note that if a two-phase lock-in amplifier is used with a noisy input, the residual noise outputs from the two phase-sensitive detectors will originate respectively from the in-phase and quadrature components of the noise. The fluctuations observed at the two outputs will, in general, be uncorrelated but otherwise have similar statistical properties.

A3.2 Noise measurements

Lock-in amplifiers are often used in a noise-measurement mode where the reference frequency and low-pass filter are selected to define a narrow measurement bandwidth centered on a spectral region of interest. A "noise measurement" unit is then used to measure the r.m.s. noise output from the low-pass filter. The result is a measure of the "spot" spectral density in the immediate vicinity of the reference frequency. This is clearly an application for a fundamental-only responding lock-in system: otherwise noise "leakage" from harmonic transmission windows could seriously affect the outcome of a measurement.

The noise bandwidth of a two-section *RC* low-pass filter is:

$$B_0 = 1/\left(8T_0\right)$$

where T_0 is the selected time constant. If the noise has an r.m.s. spectral density V_N at the reference frequency, the noise appearing in the final output will have an r.m.s.value:

$$V_{\text{r.m.s}} = \frac{V_N V_F}{\sqrt{2} S_F}\left(\frac{1}{4T_0}\right)^{1/2}$$

If $V_{\text{r.m.s}}$ is measured with a noise measurement unit, the noise voltage spectral density referred to input is:

$$V_N = 2A_N V_{\text{r.m.s}} S_F \left(2T_0\right)^{1/2} / V_F$$

where A_N is a scaling factor specified for the noise measurement unit.

Lock-in amplifiers give a unique mode of measurement whereby the noise can be measured in the presence of a synchronous signal without errors due to intermodulation. In practice, this means that noise-measurement units are almost invariably a.c. coupled to ensure that d.c. components due to detected signal do not affect the measurement of the r.m.s. value of the noise output.

Signal conditioning filters

A4.1 Low-pass Filters

A4.1.1 First-order

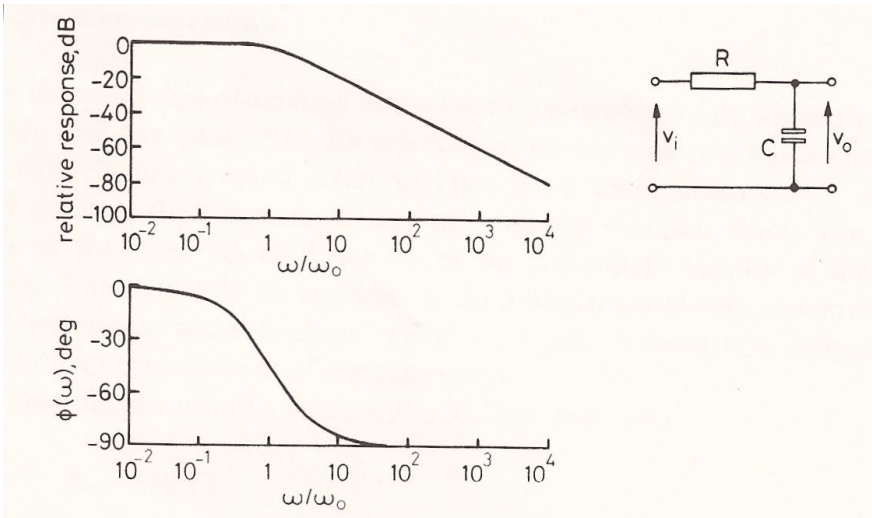

$$\omega_0 = 1/RC = 1/T_0$$

$$\left|H(j\omega)\right| = 1/\left(1+\omega^2/\omega_0^2\right)^{1/2}$$

$$\phi(\omega) = -\tan^{-1}\omega/\omega_0$$

Noise bandwidth:

$$B_N = \omega_0/4 = 1/(4T_0), \quad (\text{Hz})$$

A4.1.2 Second order

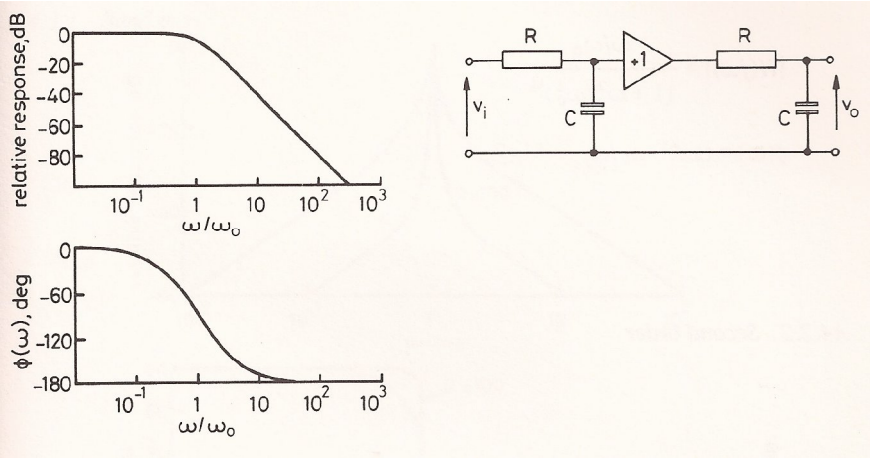

$$\omega_0 = 1/RC = 1/T_0$$

$$|H(j\omega)| = 1/(1+\omega^2/\omega_0^2)$$

$$\phi(\omega) = -2\tan^{-1}\omega/\omega_0$$

Noise bandwidth:

$$B_N = \omega_0/8 = 1/(8T_0), \quad (\text{Hz})$$

A4.2 High-pass Filters

A4.2.1First order

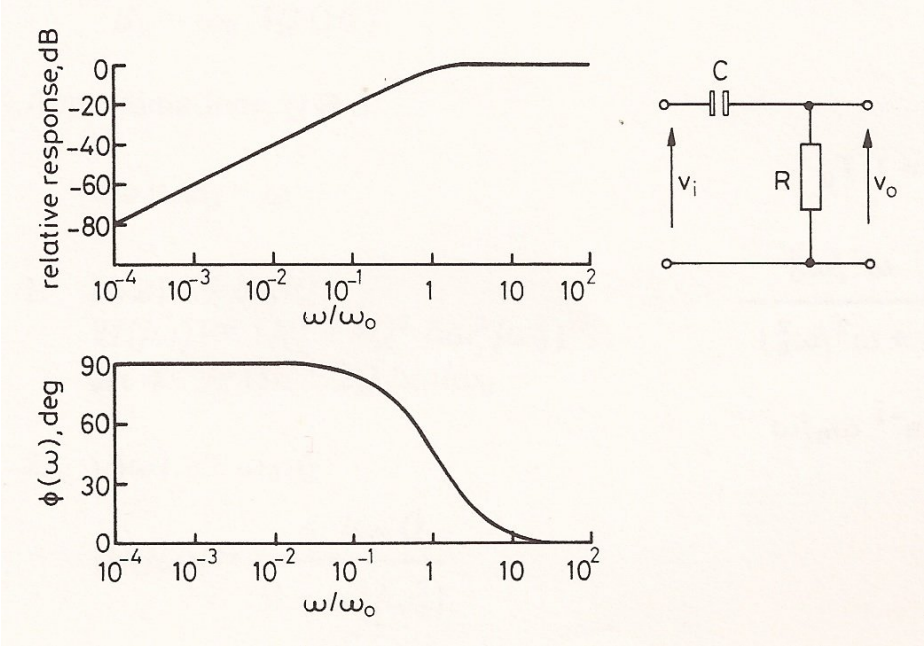

$$\omega_0 = 1/RC = 1/T_0$$

$$|H(j\omega)| = \frac{\omega/\omega_0}{(1+\omega^2/\omega_0^2)^{1/2}}$$

$$\phi(\omega) = -\tan^{-1}\omega_0/\omega$$

A4.2.2Second order

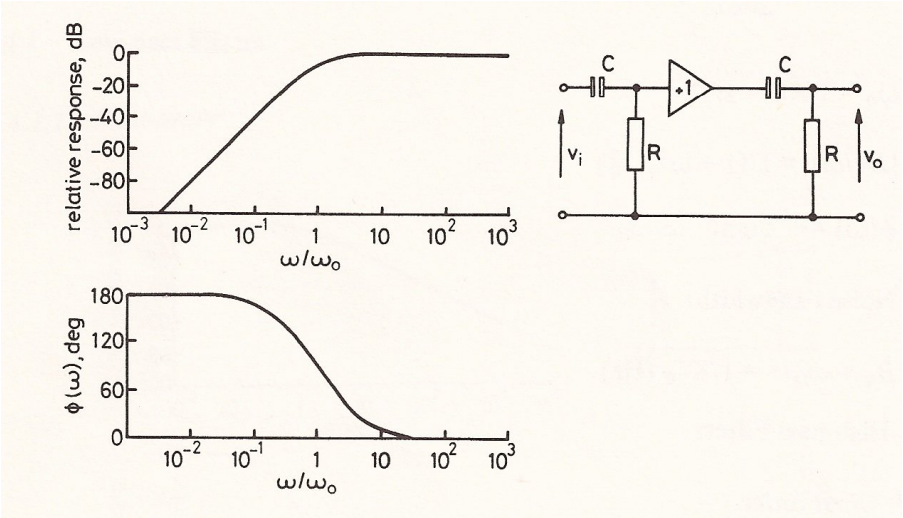

$$\omega_0 = 1/RC = 1/T_0$$

$$|H(j\omega)| = \frac{\omega/\omega_0^2}{(1+\omega^2/\omega_0^2)}$$

$$\phi(\omega) = -2\tan^{-1}\omega_0/\omega$$

A4.3 Active tuned filters

A4.3.1Band pass

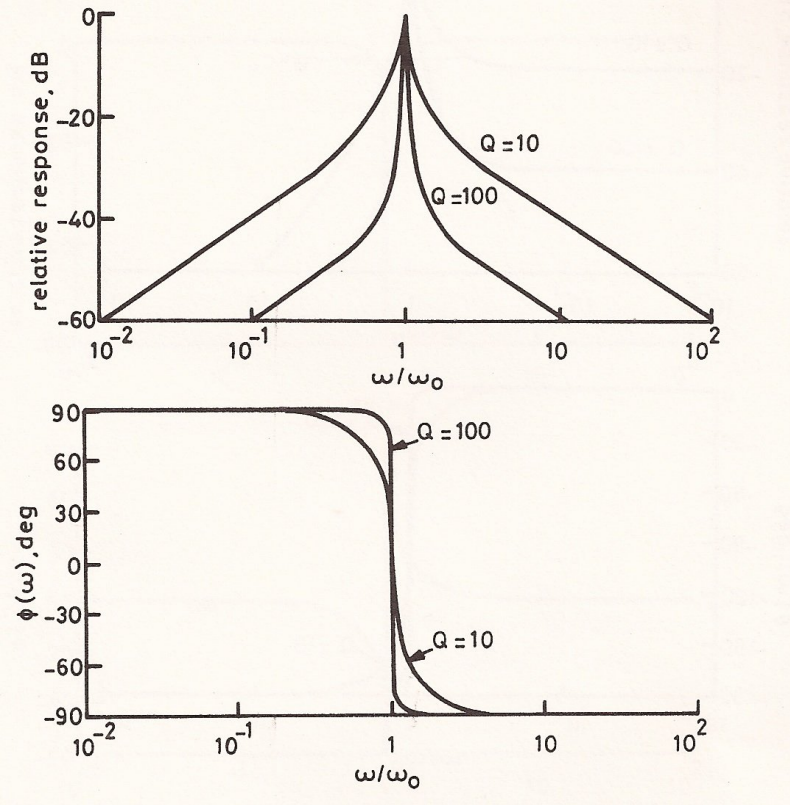

$$H(j\omega) = \frac{j\omega\omega_0/Q}{\omega_0^2 + j\omega\omega_0/Q - \omega^2}$$

–3dB bandwidth: ω_0/Q

Noise bandwidth (for $Q > \frac{1}{2}$):

$$B_N = \omega_0/(4Q), \quad (\text{Hz})$$

Approximations, $Q \geq 5$, $\Delta\omega = \omega_0 - \omega$:

1. $|\Delta\omega| << \omega_0/Q$:

$$|H(j\omega)| \approx 1/\left(1 + 4Q^2\Delta\omega^2/\omega_0^2\right)^{1/2}$$

$$\phi(\omega) \approx \tan^{-1} 2Q\Delta\omega/\omega_0$$

2. $|\Delta\omega| >> \omega_0/Q$:

$$|H(j\omega)| \approx \frac{\omega/\omega_0}{Q|1-\omega^2/\omega_0^2|}$$

A4.3.2Low-pass

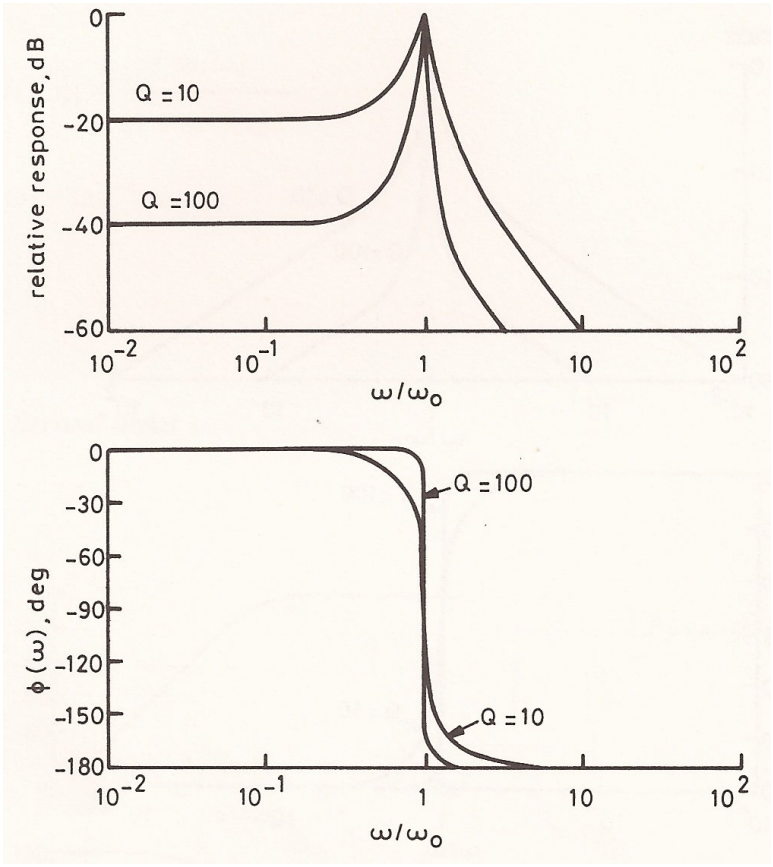

$$\left|H(\mathrm{j}\omega)\right| \approx \frac{\omega_0^2/Q}{\omega_0^2 + \mathrm{j}\omega\omega_0/Q - \omega^2}$$

–3dB bandwidth: ω_0 / Q

Noise bandwidth (for $Q > \frac{1}{2}$):

$$B_N = \omega_0/(4Q), \quad (\mathrm{Hz})$$

Approximations, $Q \geq 5, \Delta\omega = \omega_0 - \omega$:

1. $\left|\Delta\omega\right| << \omega_0/Q$

$$\left|H(\mathrm{j}\omega)\right| \approx 1/\left(1 + 4Q^2\Delta\omega^2/\omega_0^2\right)^{1/2}$$

$$\phi(\omega) \approx \tan^{-1} 2Q\Delta\omega/\omega_0 - \pi/2$$

2. $\left|\Delta\omega\right| >> \omega_0/Q$

$$\left|H(\mathrm{j}\omega)\right| \approx \frac{1}{Q\left|1 - \omega^2/\omega_0^2\right|}$$

A4.4 Active notch filter

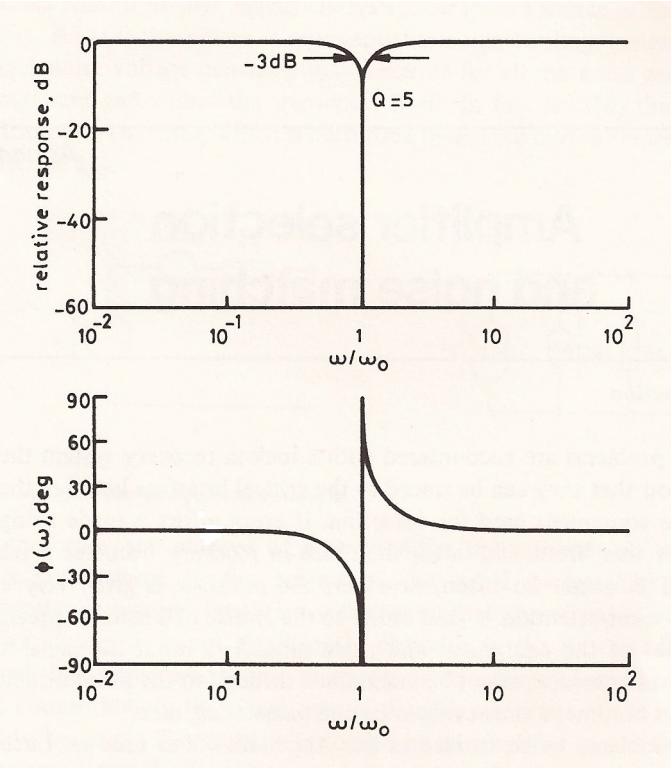

$$\left|H(\mathrm{j}\omega)\right| \approx \frac{\omega_0^2/\omega^2}{\omega_0^2 + \mathrm{j}\omega\omega_0/Q - \omega^2}$$

Notch width at –3dB points:

$\approx \omega_0 / Q$

Attenuation at $\omega = \omega_0$:

> –70 dB (typical)

APPENDIX 5

Amplifier selection and noise matching

A5.1 Introduction

If operational problems are encountered with a lock-in recovery system there is a strong likelihood that they can be traced to the critical interface between the signal source and the equipment used for detection. If every effort is made to optimize performance in the "front end" area, then lock-in recovery becomes a relatively straightforward business. So often, however, the interface is given very cursory treatment and scant attention is paid either to the choice of a suitable preamplifier or to the layout of the equipment and cable runs. As a result the signal-to-noise ratio encountered *at source* cannot be maintained through the point of detection, so measurement becomes a time-consuming and painstaking task.

The basic problems to be tacked in this Appendix are as follows. First of all, how to decide on the *type* of amplifier to be used in a given application so as to ensure that the signal is handled in the most effective and predictable way. Secondly, how to ensure that the input signal-to-noise ratio is not unduly degraded in the process of amplification, recognizing that even a "low-noise" amplifier can generate a significant amount of noise in some circumstances.

It will be assumed throughout that the principal noise limitations arise from thermal noise and shot noise. For an extension to more complicated noise models, reference should be made to a paper by Faulkner[1]. Note that design aspects of low-noise amplifiers is a topic excluded from the present treatment.

A5.2 What kind of amplifier?

We have assumed throughout our earlier discussions that the signal of interest appears in the form of an electrical signal, usually at the output of an electrical transducer. From now on we must regard this as a signal source and we shall find it convenient to represent it in the form of a circuit *model.* This is a necessary step if we are to consider the effect of making external connections.

The exact model may be more or less complex, but in many practical situations it is sufficient to use the Thevenin or Norton forms shown in Fig. A5.1 These basic forms remind us that signals always appear from a source of finite inpedance Z_s. In Fig. A5.1(a) the source is represented as a signal voltage generator v_s and the additional noise voltage generator v_{Ns} accounts for all the noise generated within the experiment and within the transducer itself. In Fig. A5.1(b) the signal appears in the form of a current i_s which is perturbed by a noise current represented here as the generator i_{Ns}.

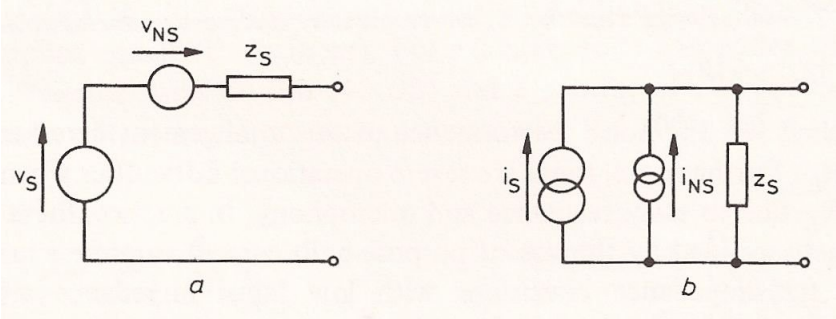

Fig. A5.1 Signal source equivalent circuits

In either case, the purpose of a preamplifier is to provide an output voltage which is proportional to the output of the signal source. The choice of an appropriately "low-noise" amplifier will ensure that the signal-to-noise ratio encountered at source is not significantly degraded in the process. It must be remembered that, while we are free to choose from a range of amplifiers or to make external connections to the signal source, the characteristics of the source must be assumed to be fixed. The problem is to choose an amplifier to suit the source, not the other way around!

In general, it is possible to define the characteristics of an amplifier to ensure that the final output depends on v_s or i_s alone, rather than on some combination of v_s or i_s with Z_s. For example, with a voltage source such as Fig. A5.1(a) it is sufficient to use an amplifier in which the input inpedance has magnitude $|Z_{in}| >> |Z_s|$. This will normally be specified as a voltage amplifier having a well-defined voltage gain over the frequency range of interest.

In the case of the current source of Fig. A5.1(b) we require an amplifier with a very *low* input inpedance compared with Z_s in order to measure the output current independently of Z_s. Such an amplifier would normally deliver an output voltage which is proportional to i_s and so is often referred to as a *transimpedance* amplifier. A common way to achieve a transimpedance amplifier is to use a voltage amplifier with a low impedance Z_L shunted across its input terminals as shown in Fig. A5.2. Those familiar with operating photomultiplier tubes will recognize this arrangement where Z_L is replaced by R_L, the anode load resistor. One reason for the popularity of this configuration is that R_L converts a hitherto "unseen" current into a more readily observable voltage variation, i_sR_L, which is subsequently amplified to give an output $A_vi_sR_L$. Dividing output by input we obtain a transimpedance A_vR_L although the overall operation is very rarely thought of in this light. Thus, increasing the load resistor is almost invariably looked upon as a means of increasing the signal voltage rather than as a means of obtaining a larger transimpedance.

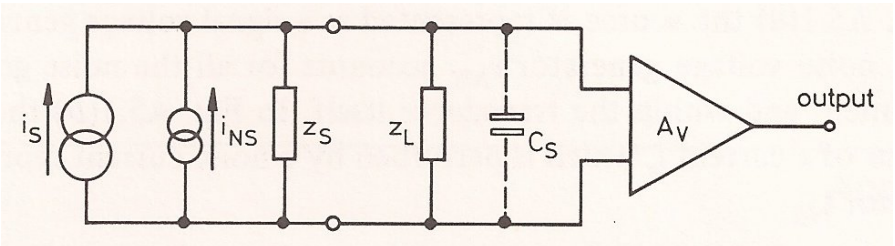

Fig. A5.2 Transimpedance amplifier. C_s represents stray reactance in the input circuit. $|Z_{in}| >> |Z_s|$

As we shall see, the noise performance of this arrangement deteriorates at low values of R_L. Furthermore, there are severe operational difficulties when using high values of R_L due to stray reactance and microphony. In practice, these difficulties can be largely avoided by the use of purpose-built current amplifiers in which high values of transimpedance consistent with low input inpedance are obtained through the use of parallel feedback.

For a given noise performance with high-impedance sources such as photomultipliers, current amplifiers can give much improved handling characteristics in terms of gain stability and relative freedom from "cable" effects. These characteristics are reviewed in Section A5.4, with special reference to photometric measurements.

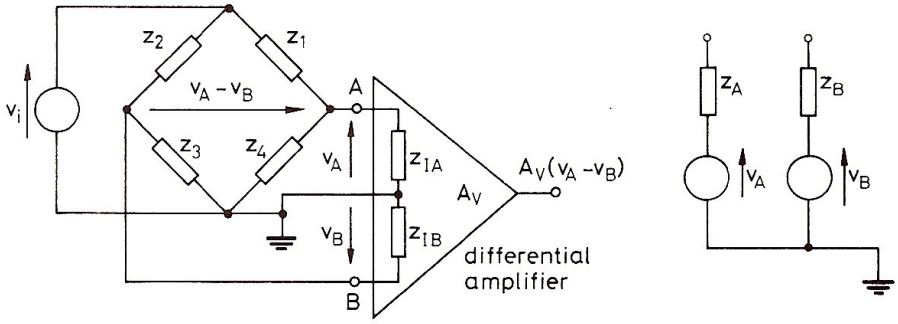

Fig. A5.3 (a) Application for a differential amplifier; (b) equivalent circuit of source. $Z_A = Z_2 // Z_3$; $Z_B = Z_1 // Z_4$

Finally, let us look at another type of voltage source exemplified by the bridge circuit shown in Fig. A5.3. Here, the signal of interest appears as the difference in potential between two points in the bridge where neither point is at ground potential. This gives us a typical application for a *differential* voltage amplifier connected as in Fig. A5.3(a). The usual arrangement is that the impedance of each amplifier input is much larger than the source inpedance presented by the bridge. This can be found by applying Thevenin's theorem to obtain the source equivalent circuit shown in Fig. A5.3(b). When the output inpedances Z_A and Z_B are identical the bridge is said to behave as a *balanced* source (not to be confused with a balanced bridge). In an unbalanced source there may be a large difference between the impedances of the two arms; however, the output inpedances are usually affected only slightly by the small adjustments which are made to the bridge at its null point.

A differential amplifier has three input terminals: A, B and ground. A voltage applied between terminals A and B is called a series or differential mode voltage. The mean voltage of A and B with respect to ground is called the common-mode voltage. A prime specification of a differential amplifier is its common-mode rejection ratio (c.m.r.r.) which gives the ratio of the series-mode gain to the common-mode gain. C.M.R.R. thus measures the ability of a differential amplifier to reject a voltage applied equally to its inputs. For example, for an amplifier with a series mode or differential gain of 100 (40 dB) and a c.m.r.r. of 10^5 (100 dB), a 1V common-mode voltage would produce an output of $1\text{ V} \times 100 \div 10^5 = 1\text{ mV}$.

C.M.R.R. is usually specified at a midband frequency, say 1 kHz, and will be in excess of 120 dB for a good-quality amplifier. Rejection falls with increasing frequency and a front-panel adjustment is often provided to maximize rejection at a frequency of interest.

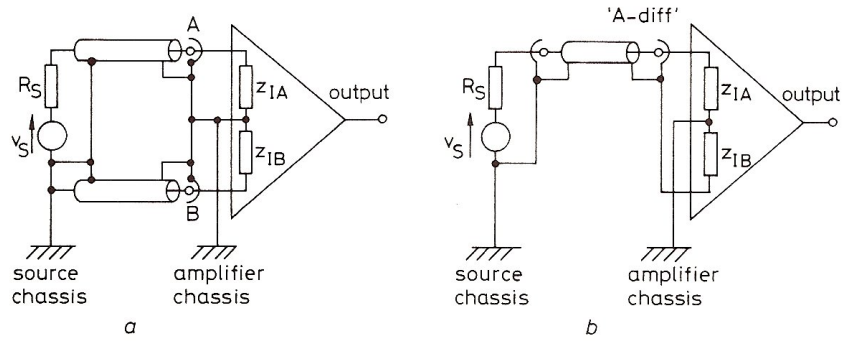

Fig. A5.4 (a) Differential with single-ended source; (b) alternative configuration using a single cable and an amplifier switched to "A-diff" mode

Differential amplifiers have an important role to play in suppressing ground loops in measurement systems. For this reason they are often specified for use with single-ended voltage sources as shown in Fig. A5.4(a). This arrangement is discussed further in Appendix 6. To facilitate connections with BNC terminations, some amplifiers incorporate a switch position labelled "A-diff" whereby the connections illustrated in Fig. A5.4(b) are made automatically. If the differential amplifier has identical input impedances on inputs A and B the inputs are said to be *balanced*. Other amplifiers offer a *pseudo-differential* or *unbalanced* input where a single input connector is wired as shown in Fig. A5.4(b) but the two input impedances are not the same. In this case, the common-mode rejection ratio is not so spectacular (usually around 80 dB), but it is possible to achieve moderate differential performance for ground-loop suppression consistent with extremely low noise. "True" differential amplifiers are generally 3 dB more noisy than their single-ended counterparts and are normally used where ultra-low-noise performance is not required. In practice, the increased immunity of a true differential stage to common-mode inputs may outweigh its additional noise contribution, and this is usually the preferred configuration for "general purpose" amplifiers.

A5.3 Noise in voltage amplifiers

A5.3.1Introduction

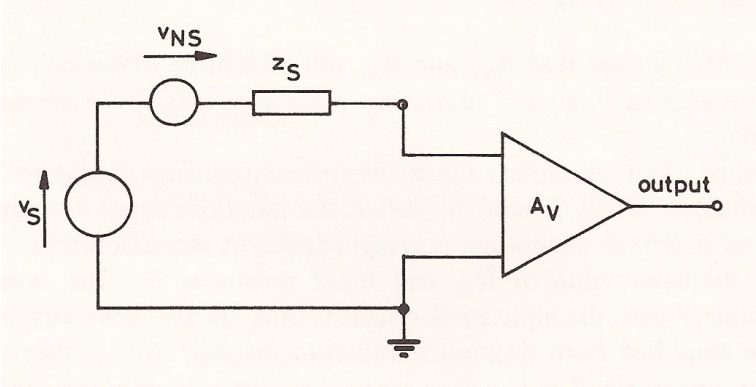

Fig. A5.5 Voltage source with amplifier

We begin with Fig. A5.5, which shows a voltage amplifier connected to a signal source. The entire source noise is accounted for by the random voltage generator

v_{Ns} which has spectral density $W(f_0)$ in the vicinity of the signal frequency f_0. The source signal-to-noise ratio measured in a small bandwidth Δf centered on f_0 is therefore

$$SNR_I = \frac{\overline{v_s^2}}{W(f_0)\Delta f}$$

We shall now assume that the signal originates in a linear passive device and that the source inpedance is resistive with value R_s over the frequency range of interest. In this important case the limitation at source is due to thermal noise so that the best possible value of source signal-to-noise ratio is

$$SNR_I = \overline{v_s^2}/(4kTR_s\Delta f)$$

where k is Boltzmann's constant and T the equilibrium temperature.

The output of the amplifier would, ideally, be an amplified version of the total input from the signal source. In practice, we must allow for noise generated within the amplifier which gives rise to an additional output fluctuation with mean-square value $\overline{v_A^2}$. The output signal-to-noise ratio is therefore less than SNR_I, and is given by:

$$SNR_0 = \frac{A_v^2\overline{v_s^2}}{\overline{v_A^2} + A_v^2 4kTR_s\Delta f}$$

where A_v is the gain of the amplifier at the signal frequency.

We now define the noise figure of the amplifying system

$$F = \frac{\text{best possible } SNR_0}{\text{actual } SNR_0}$$

This ratio will always be greater than unity for any real combination of voltage source and amplifier. In the present example, the noise figure takes the form:

$$F = 1 + \frac{\overline{v_A^2}}{A_v^2 4kTR_s\Delta f}$$

Let us now turn to the noise model shown in Fig. A5.6(a) which will enable us to predict the behaviour of the amplifier under a wide range of operating conditions.

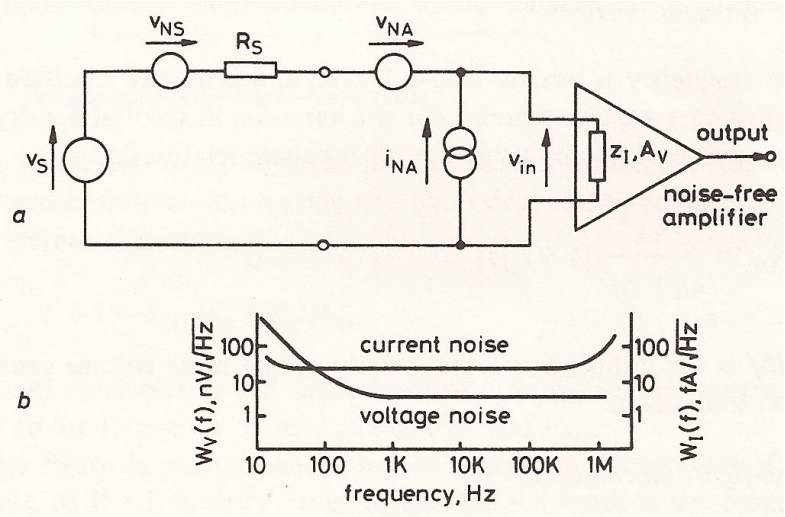

Fig. A5.6 (a) Noise model for a voltage amplifier (b) Typical spectral densities of the noise generators v_{NA} and i_{NA}

Here, the total noise of the amplifier is attributed to a pair of random-noise generators connected at its input. As is usual in such models, the amplifier itself, including the input impedance Z_I, is assumed to be noise-free. In this representation, it is clear that the signal is in competition with the amplifier noise generators v_{NA} and i_{NA}. in addition to the noise associated with the source. A fully documented voltage amplifier will have v_{NA} and i_{NA} specified in terms of their r.m.s. spectral densities over the entire frequency range of the amplifier. Fig A.5.6(b) gives an example which is typical of modern amplifiers using a j.f.e.t. input stage.

An alternative presentation which proves to be extremely useful in practicc is derived as follows. We note that the mean-square fluctuations $\overline{v_{NA}^2}$ and $\overline{i_{NA}^2}$ appearing in a bandwidth Δf centred on any frequency of interest can always be associated with *equivalent noise resistances* R_{Nv} and R_{Ni} defined by

$$R_{Nv} = \frac{\overline{v_{NA}^2}}{4kT\Delta f}$$

$$R_{Ni} = 4kT\Delta f / \overline{i_{NA}^2}$$

From Fig. A5.6(b) we see that R_{Nv} and R_{Ni} will take more or less constant values over several decades of frequency, deviating at the extremes of the operating range of the amplifier.

In the case of j.f.e.t. amplifiers the current noise originates almost entirely with the passive resistor which is used to define the amplifier input resistance. As a result, we find a virtual one-to-one correspondence in manufacturer's catalogues between the midband value of R_{Ni} and input resistance R_I. The noise of the amplifier measured with the input open-circuit is thus, for the most part, due to the thermal noise amplified from its input termination resistor. At the other end of the scale, the short-circuit noise gives a measure of the noise-voltage generator V_{NA} but here the results depend very much on the selection of input transistors and on the circuit configuration. A common feature is that the voltage noise exhibits a flicker-noise dependence at frequencies below the flicker-noise corner frequency (see Appendix 2).

The corner frequency is usually below 1kHz, and is usually specified by manufacturers. In this case we can account for the variation in spectral density and find the appropriate value of R_{Nv} by using the approximate relationship:

$$R_{Nv} = \frac{\overline{v_{NA}^2}}{4kT\Delta f}\left[1 + f_c / f\right]$$

Where $\overline{v_{NA}^2} / \Delta f$ is the midband spectral density of the noise voltage generator and f_c is the corner frequency.

A5.3.2Noise-figure calculations

We shall use our amplifier noise model to calculate the output signal-to-noise ratio when the source is limited by the thermal noise of the source resistor.

To do this it is helpful to transform the input circuit of Fig. A5.6(a) to obtain the modified noise equivalent circuit of Fig.A5.7. This shows clearly how the contribution of i_{NA} depends on the source resistance R_s. We shall assume that v_{NA} and i_{NA} are independent noise sources (that is they exhibit no correlation) and that they give rise to mean-square fluctuations $\overline{v_{NA}^2}$ and $\overline{i_{NA}^2}$ in a frequency

interval Δf centred on the signal frequency. The signal then appears in association with a total fluctuation

$$v_T^2 = 4kTR_s\Delta f + \overline{v_{NA}^2} + R_s^2\overline{i_{NA}^2}$$

and the signal-to-noise ratio measured at the amplifier output becomes

$$SNR_0 = \overline{v_s^2}/[4kTR_s\Delta f + \overline{v_{NA}^2} + R_s^2\overline{i_{NA}^2}]$$

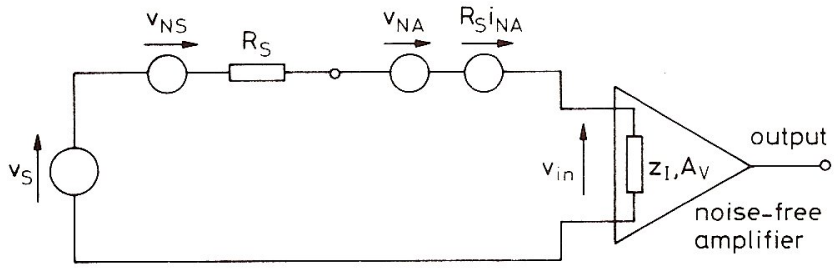

Fig. A5.7 Transformed noise-equivalent circuit

An ideal amplifier would give an output signal-to-noise ratio equal to the value measured at source, $\overline{v_s^2}/4kTR_s\Delta f$. The actual value is therefore worse by a factor

$$F = \frac{\text{best possible } SNR_0}{\text{actual } SNR_0}$$

$$= 1 + \frac{\overline{v_{NA}^2} + R_s^2\overline{i_{NA}^2}}{4kTR_s\Delta f}$$

With our particular amplifier noise model, the expression for noise figure can be put into much simpler form using the equivalent noise resistances defined in the previous section. The result is

$$F = 1 + R_{Nv}/R_s + R_s/R_{Ni}$$

which shows more clearly the dependence of F on the source resistance R_s. Also, F is subject to the frequency dependence of R_{Nv} and R_{Ni}.

If noise figure is plotted versus source resistance, using values of R_{Nv} and R_{Ni} appropriate to the frequency range of interest, the result is the parabolic curve of Fig. A5.8 which exhibits a minimum value for a value of source resistance given by $R_s = \sqrt{R_{Nv}R_{Ni}}$.

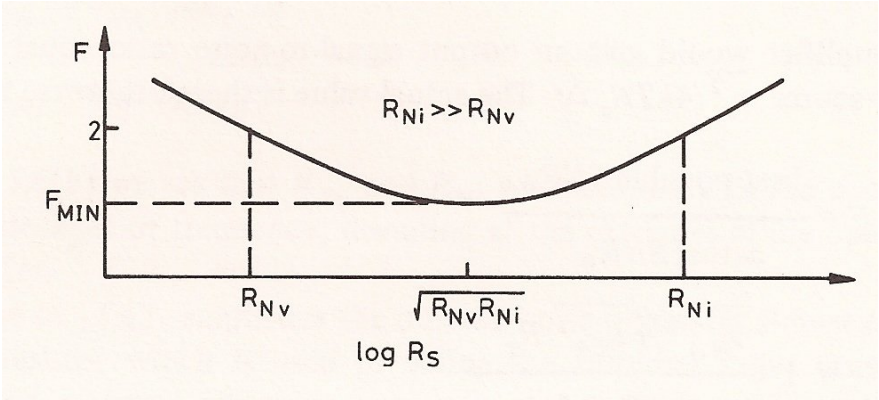

Fig. A5.8 Dependence of noise figure on source resistance.

The rise in noise figure for values of R_s less than R_{Nv} is a reminder that we cannot expect an amplifier to generate less noise than the thermal noise of an arbitrarily small source resistance. The noise figure similarly increases as R_s exceeds R_{Ni}: from the remarks made in the previous section this would normally correspond to operating a voltage amplifier from a source resistance which is greater than the amplifier input resistance.

It is evident from Fig. A5.8 that the noise-figure graph has a very broad minimum when $R_{Ni} >> R_{Nv}$. Under this condition we obtain a noise figure of 3 dB (F = 2) when $R_s = R_{Nv}$ or when $R_s = R_{Ni,}$ and a value of $F \cong 1$ for $R_s = \sqrt{R_{Nv} R_{Ni}}$.

Although it is instructive to observe how the noise figure of a given amplifier varies with source resistance, in practice we are usually faced with a fixed value of source resistance. We must then choose an amplifier from a wide range of competing devices which gives an acceptable noise figure. Any amplifier which achieves this end with a noise figure of less than 3 dB can be said to be "low noise" within the context of a given experiment, and an amplifier which is capable of giving this performance over a wide range of source resistance is said to have a *high figure of merit, M,* defined by

$$M = \sqrt{R_{Ni} / R_{Nv}}$$

Modern j.f.e.t. amplifiers have figures of merit in the range 100 to 1000 and they can be roughly classified according to the lowest value of source resistance which can be handled with an acceptable noise figure. Thus, an amplifier catalogued as "low noise" would normally be useful for source resistances as low as 1 kΩ (voltage noise of $4\ \text{nV}/\sqrt{\text{Hz}}$ at midband) while "ultra low-noise" units extend the useful range to 40 Ω or 50 Ω (voltage noise of $800\ \text{pV}/\sqrt{\text{Hz}}$ at midband).

A5.3.3 Minimum noise figure and optimum source resistance

The value of source resistance which minimizes the noise figure is known as the *optimum source resistance*:

$$R_{opt} = \sqrt{R_{Nv} R_{Ni}}$$

The minimum noise figure obtained with $R_s = R_{opt}$ is:

$$F_{MIN} = 1 + 2\sqrt{R_{Nv} / R_{Ni}} = 1 + 2/M$$

For practical purposes we can say that a noise figure of 1 dB (F = 1.26) is indistinguishable from the best possible figure of 0 dB. Since figures of merit of 100 and greater are obtainable, the minimum noise figure is easily achieved when R_s falls in the correct range. More to the point, however, we see that noise figures indistinguishable from the ideal can be obtained from a wide range of source resistances - even when R_s differs from R_{opt} by an order of magnitude - as shown in the first example below.

Example 1

A low level signal is to be measured from a source of 10 kΩ resistance at a frequency of 5 kHz. An amplifier is available with the following specification:

r.m.s. noise voltage density ($f \geq 1$ kHz):

$$4\ \text{nV}/\sqrt{\text{Hz}}, \quad R_{Nv} = 1\ \text{k}\Omega$$

r.m.s. noise current density

$$14\ \text{fA}/\sqrt{\text{Hz}}, \quad R_{Ni} = 100\ \text{M}\Omega$$

What is the noise figure that can be achieved with this combination?

The noise figure is given by:

$$F = 1 + R_{Nv} / R_s + R_s / R_{Ni}$$

$$= 1 + 0.1 + 10^{-5}$$

$$= 1.1 \text{ (0.4 dB)}$$

Let us now calculate the minimum noise figure which can be obtained using this amplifier in the same frequency range but with the optimum value of source resistance. This is

$$F_{MIN} = 1 + 2\sqrt{R_{Nv} / R_{Ni}}$$

$$= 1.006 \text{ (0.27 dB)}$$

which is obtained at a value of source resistance given by

$$R_{opt} = \sqrt{R_{Nv} R_{Ni}}$$

$$= 316 \text{ k}\Omega$$

If the signal is sufficiently strong that a degradation of 3 dB in signal-to-noise ratio can be tolerated, this same amplifier will be suitable for sources with resistances in the range 1 $\text{k}\Omega$ to 100 $\text{M}\Omega$.

Example 2

A signal of 100 nV r.m.s. is to be measured from a source of resistance 100 Ω in a bandwidth of 1 kHz using the same amplifier as in example 1.

In this case the system will have a noise figure

$$F = 1 + 10 + 10^{-6}$$

$$= 11 \text{ (10.4 dB)}$$

The r.m.s. noise voltage associated with a source resistance of x kΩ at laboratory temperature is (Appendix 2):

$$4\sqrt{x} \text{ nV}/\sqrt{\text{Hz}}$$

Hence the input signal-to-noise ratio is

$$SNR_i = \frac{(100 \times 10^{-9})^2}{16.10^{-18} \times 0.1 \times \Delta f}, \quad \Delta f = 1 \text{ kHz}$$

$$= 6.25 \text{ (8 dB)}$$

which will be reduced to 6.25/11 when the signal is amplified.

There is a clear case for seeking an amplifier with better noise performance

Suppose now, however, that the signal appears at a level of 1 μV r.m.s. The input signal-to-noise ratio is now increased to

$$SNR_i = 625 \text{ (28 dB)}$$

In this case an amplifier noise figure of 10 dB or so would reduce the output signal-to-noise ratio to about 18 dB, which might be considered quite adequate if the signal is to be measured in a recovery system. A decision to select an "ultra low-noise" amplifier with $R_{Nv} = 100\ \Omega$ or less may then be uneconomical provided that 1 μV r.m.s. represents the minimum value of the signal for all time. If, at a later stage, the signal amplitude is likely to be reduced beyond this value, then the question of amplifier noise will undoubtedly be raised again.

Finally it should be noted that these examples are for operation at a fixed frequency, using the values of R_{Nv} and R_{Ni} appropriate to that frequency. If operation over a wider frequency range is envisaged, then more information is required. Fortunately, this is usually available, as discussed in the following section.

A5.3.4Noise-figure contours

Since noise figure depends upon frequency in a fairly complicated way, most manufacturers elect to present their data graphically in the form of *noise-figure contours.*

Figure A5.9 shows a single contour, the 3 dB contour, drawn against axes labelled with source resistance and frequency on logarithmic scales. The shape of the contour is derived as follows: first of all, the regions (i) and (ii). These define the lower and upper limits of R_s required to give a noise figure of 3 dB at midband. They thus coincide with the midband values of R_{Nv} and R_{Ni}. The rise in the lower contour in region (iii) results from the rise in R_{Nv} at low frequencies due to flicker-noise effects in the amplifier, and shows that the value of R_s required to maintain a 3 dB noise figure becomes progressively larger as the operating frequency is reduced.

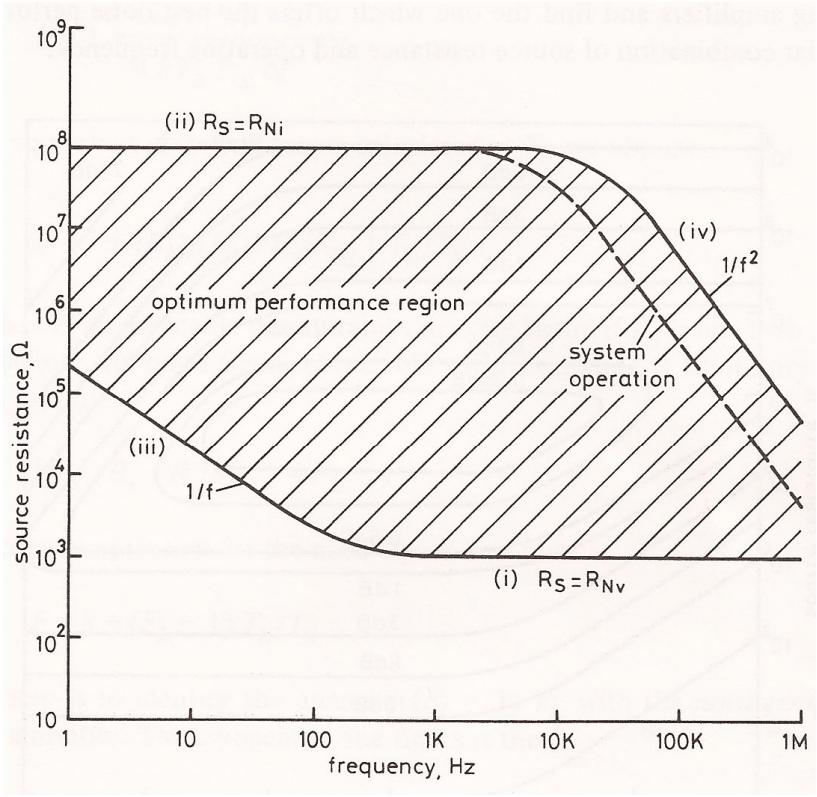

Fig. A5.9 The 3 dB noise-figure contour for a low-noise voltage amplifier

The sloping characteristic in region (iv) indicates that R_{Ni} is, in fact, *reduced* at high frequencies and that R_s must be reduced in proportion if the noise figure is to be held at the midband value of 3 dB. This is one area where the contours are particularly useful since the high-frequency cut-off depends on the "noise capacitance" of the amplifier which may not otherwise be specified. We can be sure, however, that if the amplifier input is heavily loaded with cable capacitance, the turn-over in the upper contour will shift to lower frequencies as indicated by the broken line appropriate to "system" operation.

The area enclosed by the 3 dB contour is often called the "optimum performance" region. Its vertical extent is maximized by selecting an amplifier with a high figure of merit, but this should be consistent with a low value of R_{Nv} if optimum performance is required from low source resistances. In many voltage-amplifier applications where the source resistance is less than 1 MΩ, the loss of performance in region (iv) is not normally significant. However, the turn-over frequency can be as low as 1 kHz for amplifiers with extremely high input resistance, of the order of 1 GΩ.

A complete set of contours for a general-purpose low-noise voltage amplifier is shown in Fig. A5.10 exactly in the form which might be encountered in a manufacturer's catalogue. The contours provide the means for a researcher to compare competing amplifiers and find the one which offers the best noise performance for a particular combination of source resistance and operating frequency.

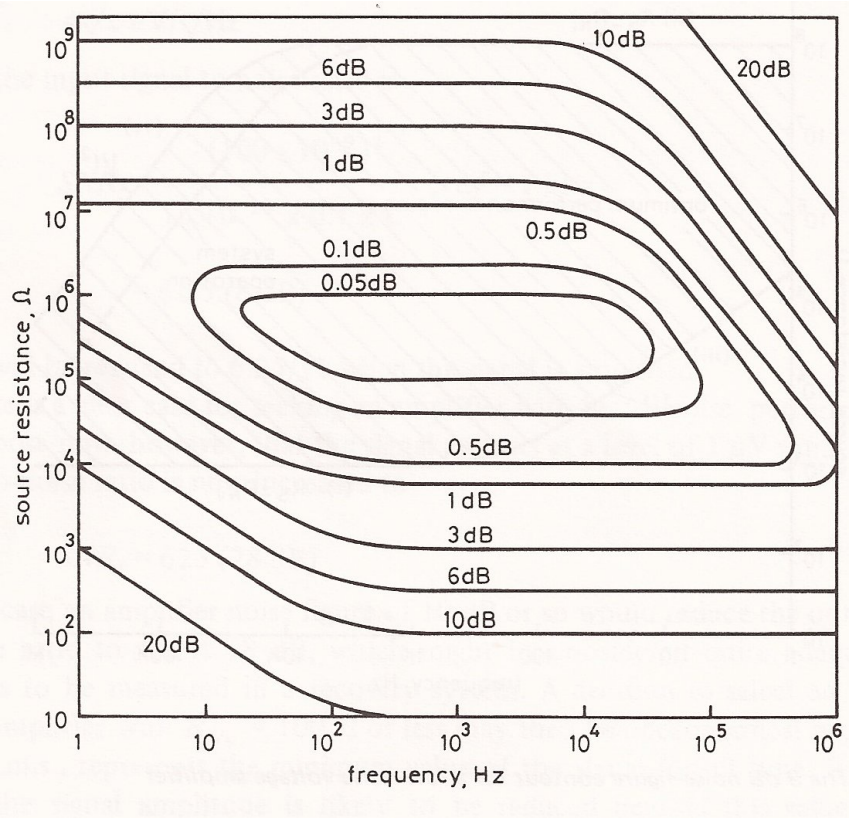

Fig. A5.10 Typical noise-figure contours

Alternatively, if an amplifier is available and there is sufficient latitude in, say, the choice of experimental frequency, it may be possible to arrange to operate within the optimum performance region of the amplifier. For example, if an optical detector provides a signal from a source resistance of 10 kΩ and the amplifier contours are those given by Fig. A5.10, we find that changing the optical chopping frequency from 10 Hz to 100 Hz brings an improvement in noise figure from 3 dB to less than 1 dB even though both frequencies lie below the flicker-noise corner frequency of the amplifier.

A5.3.5 Cryogenic sources

The noise figure data supplied by manufacturers almost invariably refer to the source and amplifier at normal laboratory temperatures. Let us now return to our original definition of noise figure and rework the results for the more general case

where the source is at a different temperature to the amplifier. We shall assume that v_{NA} and i_{NA} are specified at laboratory temperature T_L, say 290 K, and represent the source temperature by T_s. The noise figure is now:

$$F = 1 + \frac{\overline{v_{NA}^2} + \overline{i_{NA}^2} R_s^2}{4kT_s R_s \Delta f}$$

Using the equivalent noise resistances calculated at T_L we obtain:

$$F = 1 + \left[R_{Nv} / R_s + R_s / R_{Ni} \right] T_L / T_S$$

which indicates an inevitable deterioration in noise figure if T_s is less than T_L.

If we denote the noise figure obtainable with the source at laboratory temperature by F_L, then

$$\left[R_{Nv} / R_s + R_s / R_{Ni} \right] = F_L - 1$$

and the general expression for the noise figure becomes:

$$F = 1 + \left(F_L - 1 \right) T_L / T_S$$

The next step is to identify the quantity $\left(F_L - 1 \right) T_L$ with the *noise temperature,* T_e, of the amplifier. The cryogenic noise figure is then

$$F = 1 + T_e / T_s$$

Thus, we find that to give a noise figure of 2 (3 dB) with a cryogenic source, the noise temperature of the amplifier must equal the temperature of the source.

Unfortunately, low-frequency voltage amplifiers are rarely specified directly in terms of noise temperature. The following examples show the sort of calculation which must usually be undertaken.

Example 1

An amplifier has a noise figure of 2 dB when operated with an optical detector at room temperature (F_L = 1.58). What is the achievable noise figure when operating with a detector of the same resistance at a temperature of 77 K?

We have

$$F_L = 1.58$$

so the noise figure obtainable at a source temperature of 77 K is:

$$F = 1 + (1.58 - 1) \times 290 / 77$$

$$= 3.18 \text{ (5 dB)}$$

Example 2

For a given value of source resistance, what noise figure must be achieved with a source at laboratory temperature to ensure a cryogenic noise figure of 3 dB for sources at (a) 77 K and (b) 4 K?

The amplifier should be capable of operating at a noise temperature of 77 K in the first case and 4 K in the second. The maximum acceptable noise figure with the source at laboratory temperature is then

$$F_L = 1 + T_e / 290$$

This gives (a) F_L = 1.26 (1 dB) and (b) F_L = 1.014 (0.06 dB).

In this situation it is clear that the "optimum performance" region - which is bounded by the 3dB noise-figure contour for operation with sources at laboratory temperature - is now considerably reduced in area and effectively replaced by a

smaller region bounded by the 1 dB or even the 0.05 dB contour. This places restrictions on the choice of operating frequency and defines a much tighter bound on the value of source resistance required to maintain an acceptable noise figure. We can conclude that extremely low noise figures have rather more than academic interest when cryogenic sources are involved. If the source resistance differs widely from the optimum value appropriate to a given amplifier, it will be necessary to introduce a stage of noise "matching" using a signal transformer.

A5.3.6 Transformer noise matching

The voltage noise resistance R_{Nv} of even an "ultra low-noise" amplifier may, in many cases, be too high to give an acceptable noise figure from sources either of low resistance or at low temperature. In such cases it may be necessary to resort to noise "matching" whereby the source resistance is transformed to a new value which is much closer to the optimum sources resistance of a given amplifier. It should be noted that *noise* matching is achieved in the interest of maximizing the signal-to-noise ratio at the output of an amplifier, and is quite distinct from any attempt made to maximize either the signal voltage or the signal power through *impedance* matching.

As a first step we can disregard any attempt to "transform" the source resistance by the addition of resistors between the source and the amplifier. Series resistors merely add to R_{Nv} when performing noise calculations, and parallel resistors cause a reduction in R_{Ni} and will always degrade the signal-to-noise ratio. Far from "reducing signal and noise equally" an input attenuator will always introduce noise at the expense of the signal.

The usual approach is to introduce a transformer of turns ratio n_T as shown in Fig. A5.11. We shall assume for the moment that the transformer is ideal with no loss, wide bandwidth and infinite self-inductance. The transformer reflects a voltage $n_T v_s$ into its secondary circuit and a resistance $n_T^2 R_s$. The signal-to-noise ratio at the transformer output is thus unchanged and remains at its "best possible" value while the amplifier "sees" a source of resistance $n_T^2 R_s$. By suitable choice of n_T, therefore, we can arrange for the noise matching condition:

$$n_T^2 R_s = R_{opt}$$

and so ensure that the overall system operates at its minimum noise figure.

Practical transformers can bring about a significant improvement in system performance, but, nevertheless, fall short of the ideal in almost every respect. Among the factors which must be taken into account are a reduced response when the transformer is operated outside its recommended frequency range and the effect of noise generated within the transformer itself. The latter includes the effects of vibration and the susceptibility of the transformer to pick-up, particularly at line-related frequencies.

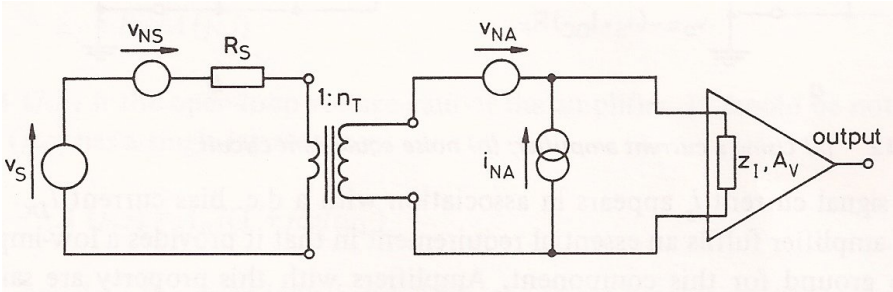

Fig. A5.11 Noise matching using a transformer

The useful frequency range of a transformer depends jointly on the source resistance and, in those with multiple tappings, on the selected turns ratio. The usual behaviour is a restriction on bandwidth when either R_s or n_T is increased; the information is most usefully presented in graphical form.

In commercial transformers the pick-up problem is reduced by packaging the transformer in a heavily screened box, while the effects of vibration and microphony are suppressed by the use of shock-absorbing mounting materials. This leaves the resistance of the windings as the main source of internally generated noise since the thermal noise of the primary coil plus the noise reflected from the secondary effectively add to the applied signal.

The noise resistance of a transformer is given in terms of the primary and secondary coil resistances R_1 and R_2 by:

$$R_T = R_1 + R_2 / n_T^2$$

It is thus possible to define a noise figure for a transformer and - as in the case of amplifiers - to present noise figure as a function of source resistance and operating frequency. Most useful of all, however, are the noise-figure contours plotted directly for a given combination of transformer and amplifier that are made available by some manufacturers.

A5.4 Noise in current amplifiers

Our interest in this section is with current amplifiers obtained by applying parallel feedback to a high-gain, low-noise voltage amplifier. A typical arrangement is shown in Fig. A5.12(a) in which the current amplifier* is connected to a high-impedance transducer modelled as an ideal current source.

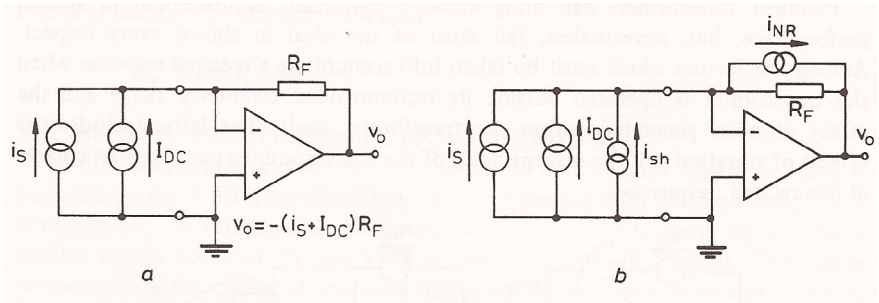

Fig. A5.12 (a) Using a current amplifier; (b) noise equivalent circuit

The current signal i_s appears in association with a d.c. bias current I_{DC} and the current amplifier fulfils an essential requirement in that it provides a low-impedance path to ground for this component. Amplifiers with this property are said to be able to "sink" a d.c. current (which may be many orders of magnitude greater than the signal current).

The dominant sources of noise are due to the shot noise of the current source and thermal noise in the feedback resistor R_F, which are included in the noise equivalent circuit of Fig. A5.12(b). If the amplifier is not to degrade the signal-to-noise ratio encountered at source, then the shot-noise contribution must exceed the thermal-noise contribution. Following the arguments developed in Section A2.4, we obtain the condition:

---

* Although strictly a transimpedance amplifier, the arrangement in Fig. A5.12(a) is usually catalogued as a current amplifier when the transimpedance is substantially real and constant over the operating frequency range. The transimpedance is given in this case directly by the feedback resistor, R_F.

$$I_{DC} \geq \frac{2kT}{qR_F}, \quad (2kT/q \approx 50 \text{ mV at } T = 290 \text{ K})$$

This defines a lower limit on I_{DC} to maintain an acceptable noise performance. At large values of I_{DC} we find a further limitation; this is given by the maximum value of bias current which can be sunk without driving the amplifier into saturation. We obtain:

$$I_{DC} \leq (V_{OUT})_{MAX} / R_F$$

and so arrive at the allowed range of I_{DC}:

$$50 \text{ mV} / R_F \leq I_{DC} \leq (V_{OUT})_{MAX} / R_F$$

Even if $(V_{OUT})_{MAX}$ were little more than 50 mV, there would always be a value of R_F which gave the required current sinking and which contributed noise not greater than the input current shot noise. In practice $(V_{OUT})_{MAX}$ is usually of the order ± 10 V. Thus, for any given value of R_F, the smallest and largest currents which can be accepted by the amplifier without, on the one hand, suffering significant noise degradation, and, on the other hand, exceeding the amplifier's current sinking capability, may be in the ratio 50 mV:10 V or 1:200.

One reason which is often cited for choosing "true" current amplifiers is their relative immunity to "cable" effects. This refers to the effects of pick-up, capacitive loading and microphony which can result when a high-impedance source is terminated by a large load resistor and connections are made via long cable lengths. When a current amplifier is used, the additional impedance introduced by such a cable is shunted by the relatively low input impedance of the amplifier given by:

$$Z_I = R_F / A(j\omega)$$

where $A(j\omega)$ is the open-loop voltage gain of the amplifier. It should be noted that when $A(j\omega)$ has a single-lag response:

$$A(j\omega) = A_0 / (1 + j\omega/\omega_1)$$

with ω_1 equal to the open-loop bandwidth, the input impedance has an inductive component and takes the general form:

$$Z_I = R + j\omega L$$

where

$$R = R_F / A_0$$

and

$$L = R_F / \omega_1 A_0$$

Although current amplifiers are particularly immune to the effect of stray capacitance on the input cable, this capacitance can have an adverse affect on noise performance at sufficiently high frequencies. To see this, we must take into account the input voltage noise generator of the amplifier v_{NA} which gives rise to an input noise current:

$$i_{Nv} = v_{NA} 2\pi f C_s$$

C_s represents the total capacitance of the source and the amplifier input. Its effect is illustrated graphically in Fig. A5.13 for the case where v_{NA} has a midband value of $4 \text{ nV}/\sqrt{\text{Hz}}$. The graph shows the value of C_s that causes an increase of

3 dB in the amplifier noise contribution as a function of feedback resistor R_F and frequency.

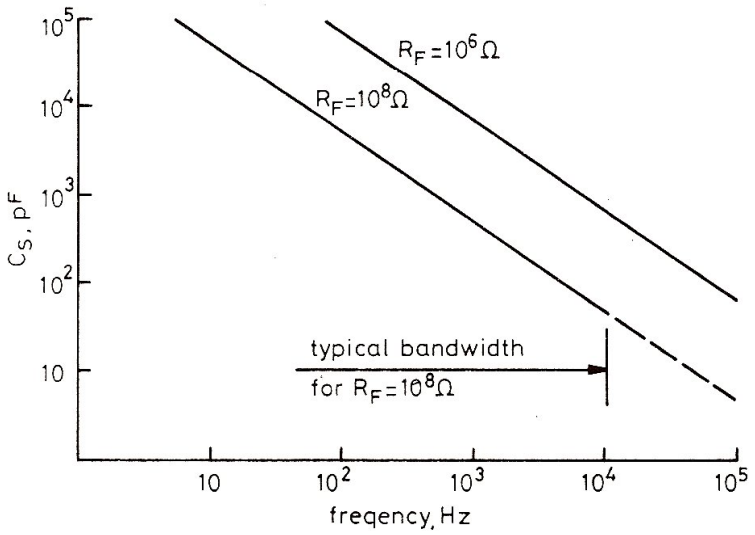

Fig. A5.13 Maximum allowed value of C_s for optimum noise performance of a current amplifier

A5.5 References and further reading

1 FAULKNER, E.A. (1975): "The principles of impedance optimisation and noise matching", *J. Phys. E: Sci. Instrum.*, 8, pp. 533-540.

2 Technical Note 101 (1077): "The use of current preamplifiers", (EG&G Brookdeal, Bracknell, England).

3 Technical |Note 243 (1976): "Noise in amplifiers", (EG&G Princeton Applied Research Corp., Princeton, NJ).

4 "Noise figure contours" (1969), (EG&G Princeton Applied Research Corp., Princeton, NJ).

Interference and ground loop suppression

A6.1 Introduction

Although consideration has been given to sources of fundamental noise in experiments and to the noise contribution of amplifiers, it is noise injected by pick-up from external sources that is usually the most troublesome in practice. In this Appendix we shall therefore be dealing with some of the problems that are met when small signals are handled in a typical laboratory environment.

A useful starting point is to list the principal mechanisms by which interference couples to experiments:

(i) capacitive pick-up;

(ii) inductive pick-up;

(iii) electromagnetic interference (e.m.i.);

(iv) high-frequency interference superimposed on mains supplies;

(v) ground loops.

Problems associated with ground loops will be left until a later stage. Otherwise, means of overcoming the first four sources of interference are generally well known and have been thoroughly documented[1,2]. These can be summarized as follows:

(a) Use screened cables to reduce capacitive "hum" pick-up between signal and power lines to suppress crosstalk between adjacent signal cables. Reinforce this approach by ensuring that low-level signal cables are routed separately from mains cords and digital highways. Reduce point-to-point capacitive pick-up within an experiment by the use of metal enclosures or fine mesh screens.

(b) Arrange for a large separation of signal lines from sources of power-frequency magnetic fields such as transformers and electric motors. Reduce the susceptibility of circuits to stray magnetic fields by eliminating large circuit loops.

    Transmit signals via screened twisted pairs where spurious voltages induced in successive small loops tend to cancel. These would normally be essential first steps before resorting to expensive solutions involving high-permeability screening. Note that lock-in amplifier construction, toroidal transformers having low external fields are almost always used in order to reduce "hum" pick-up within the instrument case.

(c) When laying out experiments it should be remembered that loops of wire act as antennas at radio frequencies and that the nature and quality of a signal ground is considerably obscured when the length of the ground path becomes comparable with a wavelength at the interference frequency[3].

The effect of electromagnetic interference in a long cable run can be suppressed by techniques that raise the r.f. impedance of the cable. For example, it is worth

investigating the effects of coiling the cable to form an r.f. choke. Other transmission-line techniques involve the use of transmission-line transformers and *coaxializers*. The most simple form consists of a few turns of screened cable wound on a ferrite toroid as illustrated in Fig. A6.1. This arrangement has the practical advantage of maintaining d.c. continuity throughout the length of the cable and is sometimes known as a *longitudinal choke*[1]. The tight coupling introduced by the winding results in a considerable attentuation of r.f. common-mode voltage but presents a low impedance to signal current. This technique can also be applied successfully when a differential signal is transmitted over a screened twisted pair[4].

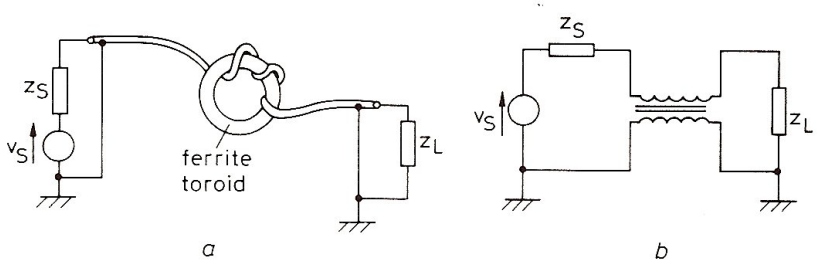

Fig. A6.1 (a) A longitudinal choke; (b) equivalent circuit

In general, the only satisfactory approach to suppressing electromagnetic interference is to systematically trace the interference source and to identify the path by which it couples to the experiment. In severe environments it may be necessary to erect a mesh screen forming a Faraday cage either around the experiment or around the offending source when this is most convenient. The screen should be earthed at one point only, using the most direct route possible.

(d) In many cases, the source of high-frequency interference can be traced to the coupling of large transients to the powerlines from pulsed lasers, thyristor controllers, laboratory ovens and other ancillary equipment used in experimental work. The solution here may be to use plug-in r.f. filters on the mains inputs of sensitive instruments to prevent transient interference appearing on instrument power supplies.

Let us now turn to the last item in our original list: ground loops. The fact is that even when detailed attention has been paid to screening and laying out cable runs, experiments can still be plagued with interference. The reason is that screened connections have finite inpedance, and so are able to support spurious voltage drops. These can give rise to severe measurement difficulties unless careful attention is paid to experiment design. Lock-in amplifier-based experiments are particularly prone to earthing problems. The result can be a large component of synchronous voltage appearing at the signal input that could be much larger than the "true" synchronous signal of interest. This aspect is discussed further in Section A6.4.

A6.2 Ground loops: single-ended amplifiers

Fig. A6.2 shows the connection of a transducer voltage source to a single-ended amplifier via a screened cable. The cable screen is securely referenced to the amplifier earthing point and is thus effective in shielding the sensitive inner conductor against capacitive pick-up from external sources.

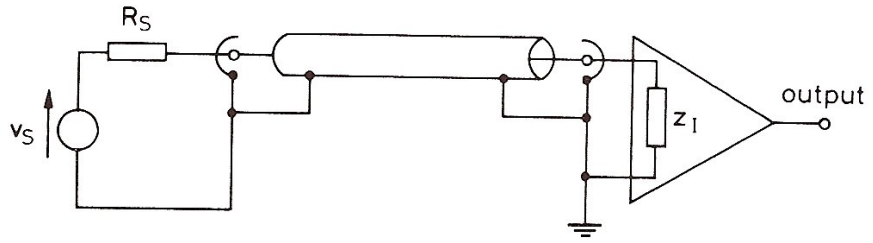

Fig. A6.2 Connection of a "floating" source and grounded amplifier

Unfortunately, it is not always possible to maintain the screen at the same potential along its entire length. When this cannot be achieved, the effectiveness of the screen is reduced because variations in screen potential become capacitively coupled to the inner conductor. Also, in some circumstances the voltage developed across the cable screen is able to add directly to the signal voltage.

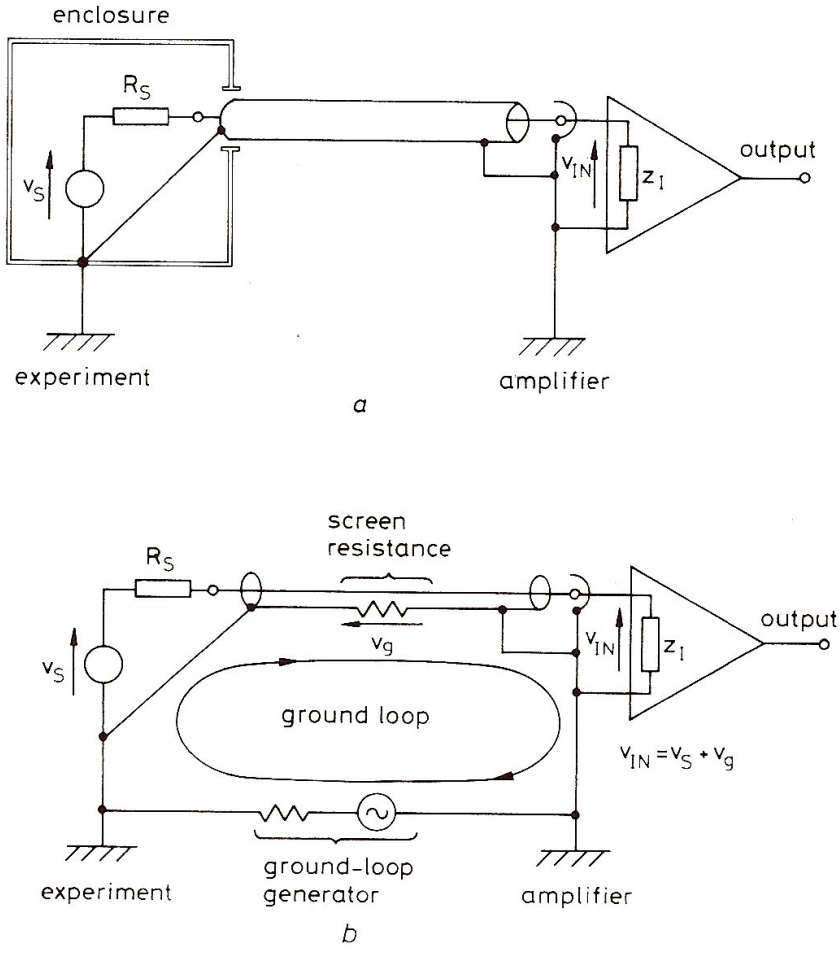

Fig. A6.3 Ground loop established when items of "grounded" equipment are interconnected

Consider, for example, the connections shown in Fig. A6.3(a). Here, the signal source is located inside a screening enclosure. Following "good practice" for optimum screening, the signal-source common and the cable screen have been connected to a single earth point to ensure that no signal currents or earth currents

flow through the enclosure. The main problem in this, or any similar, arrangement, is to define a true "wet earth" for screen connections. The use of chassis symbols with separate labels for "experiment" and "amplifier" reminds us that in an extensive laboratory installation it is not unusual to find a.c. potential differences of several hundred millivolts between adjacent chasses. Any attempt to connect these via a cable screen of finite impedance then results in a *ground loop* as indicated in Fig. A6.3(b). this loop is sensitive to any potential difference between the two chasses and is additionally susceptible to inductive coupling to stray magnetic fields. Both these effects are accounted for by the inclusion of a ground loop generator in Fig. A6.3(b) which develops a voltage drop v_g across the cable screen. Because the amplifier senses the potential difference between the screen and the inner conductor of the connecting cable, the so-called *common mode voltage*, v_g is effectively added to the signal.

This spurious input may dominate the measurement of the signal unless appropriate steps are taken. In principle, the common-mode signal can be eliminated by bringing the source and amplifier chasses to the same potential, but attempts to achieve this are rarely successful in practice. Even when units are brought into close proximity and bolted to a metal plate it is not unusual to find large potential differences between "earth" points only a few inches apart. A far better approach is therefore to investigate ways of "floating" either the source or the amplifier with a view to breaking the ground loop completely.

In the case of this source this might be achieved by using insulating bolts and washers to prevent direct contact between the transducer case and the experimental chassis. Where this is not feasible, a battery-powered preamplifier provides a reliable (and safe) way of isolating the amplifier input. An alternative and usually more convenient approach is to use a *semi-floating* amplifier in which a "float" resistor, typically in the range 50 Ω to 1 Ω, is used to provide a degree of isolation which approaches actual breaking of the ground loop.
Fig. A6.4 shows how the float resistor is inserted between the cable screen and the amplifier chassis; as a result, most of the ground loop voltage is dropped across the float resistor, leaving a relatively small fraction across the cable screen. In effect, the common-mode signal v_g is reduced by the ratio of the screen resistance (typically a few tens of milliohms) to the float resistance. Note that the reduction of the spurious voltage across the screen also results in a corresponding reduction in interference capacitively coupled from the screen to the inner conductor of the connecting cable.

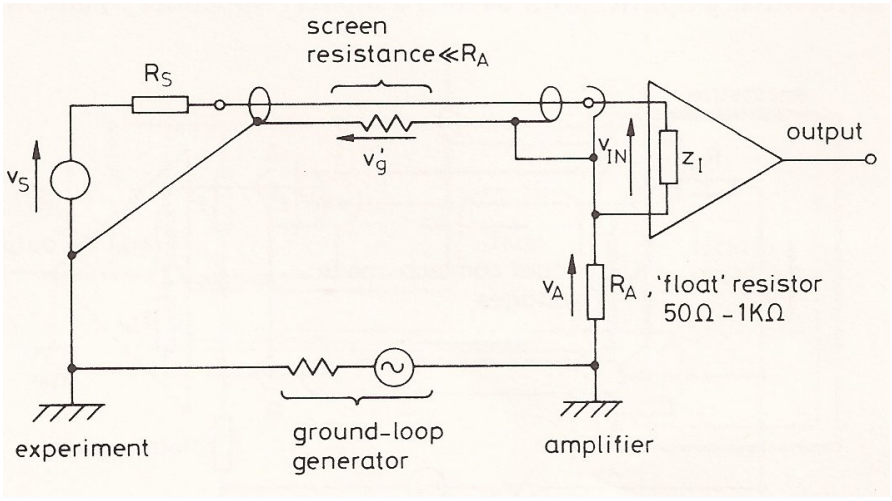

Fig. A6.4 Introduction of an amplifier "float" resistor, resulting in a much reduced common-mode votlage v_g

A6.3 Ground loops: differential amplifiers

The ground-loop suppression afforded by a semi-floating single-ended amplifier is impressive, but yet may be insufficient in some circumstances. When, for reasons of safety or practicability, it is not possible to use a floating source, residual connection problems can usually be overcome by using a differential amplifier as shown in Fig. A6.5. As before, an amplifier float resistor is used to bring about a large reduction in the spurious cable screen voltages which now appear as equal common-mode voltages across the amplifier inputs. As explained in Appendix 5, the extremely high common-mode rejection of the amplifier will then ensure suppression of ground-loop interference at power frequencies.

In order to maximize suppression it is essential to provide identical routes between source and amplifier for both cables to ensure that there is no differential pick-up in the two screens. This problem can be overcome by arranging to transmit differential signals over twisted pairs in a common screen, an approach favoured by instrumentation engineers. The symmetry of a twisted-pair connection also tends to equalize capacitive pick-up between the screen and the two conductors, and is additionally effective in reducing inductive pick-up.

The common-mode rejection ratio of a differential amplifier falls at high frequencies. Common-mode pick-up at radio frequencies should therefore be reduced as far as possible using screening and the coaxilizer techniques referred to earlier. Even at moderate interference frequencies, spurious phase shifts caused by the distributed cable capacitances acting with unequal resistances in the two paths may cause incomplete cancellation of common-mode voltages. An improvement will usually be obtained when a fully balanced source such as an a.c. bridge is used with a "true" differential amplifier with balanced inputs (Appendix 5) and matched cable lengths.

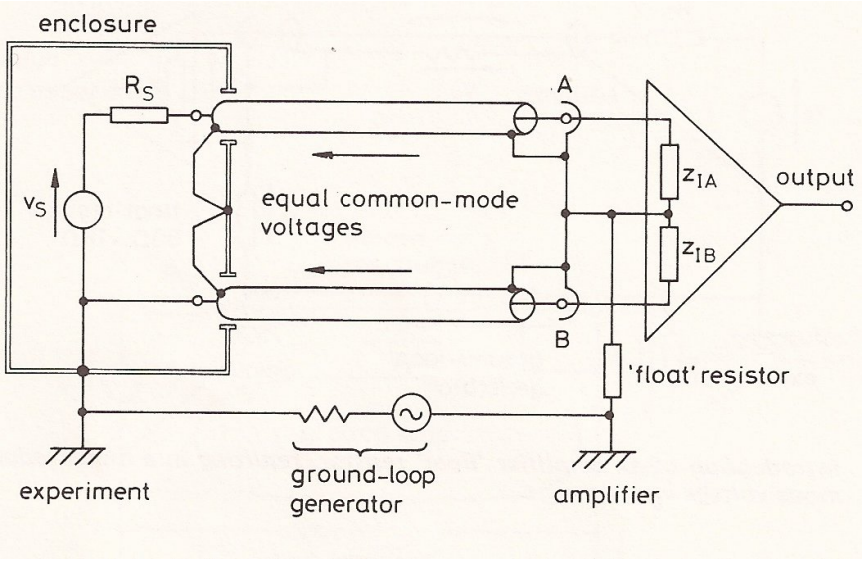

Fig. A6.5 Using a differential amplifier to overcome grounding problems

A6.4 Ground loops and lock-in recovery

Careless connection of signal and reference cables to a lock-in amplifier can lead to ground-loop problems over and above those described so far.

In most signal-recovery experiments, an oscillator is used as both an excitation and reference source, while the signal is taken from a "single-ended" transducer output. Fig. A6.6 gives an example where the oscillator and transducer output are

strapped to the chassis of the experiment with direct connections made to the reference and signal inputs of a lock-in amplifier. The impedance Z_E represents the load provided by the excitation circuit to the experiment. To take a specific example, the oscillator could provide the drive to a vibration or "shaker" table, while the signal output is derived from a vibration transducer mounted on the device under test. In this case, the drive current could be several orders of magnitude greater than the current flowing in either the reference or signal circuits.

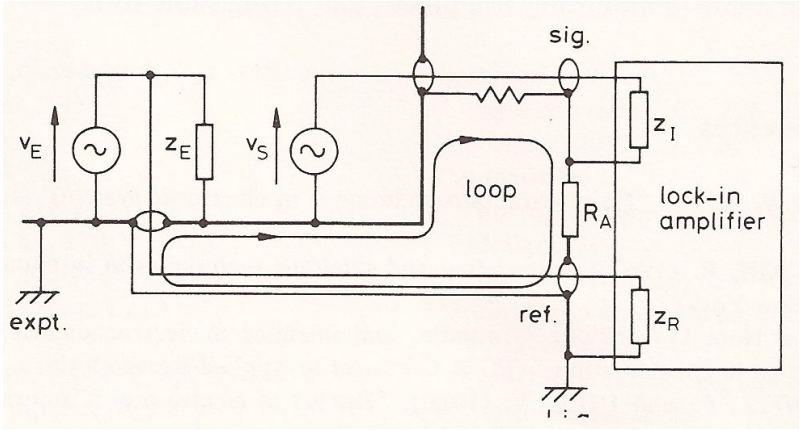

Fig. A6.6 Indiscriminate connections in a lock-in amplifier-based experiment causing a synchronous loop

Problems will arise in practice with the arrangement shown because the return path from Z_E to the excitation oscillator is shunted by a second path formed by the screen connections on the reference and signal connection cables. A fraction of the drive current is thus able to circulate in this path and generate a *synchronous* voltage drop across the signal screen in series with the signal voltage of interest. Although the amplifier "float" resistance R_A will attenuate the voltage considerably, the spurious voltage could well be greater than the signal voltage. The fact that spurious voltage is also synchronous with the applied reference would severely restrict the range over which measurements could usefully be performed.

Note that if the drive load were omitted completely, the signal screen would continue to provide a return path for a fraction of the current flowing in the reference circuit. Fortunately, the reference current is limited by the input

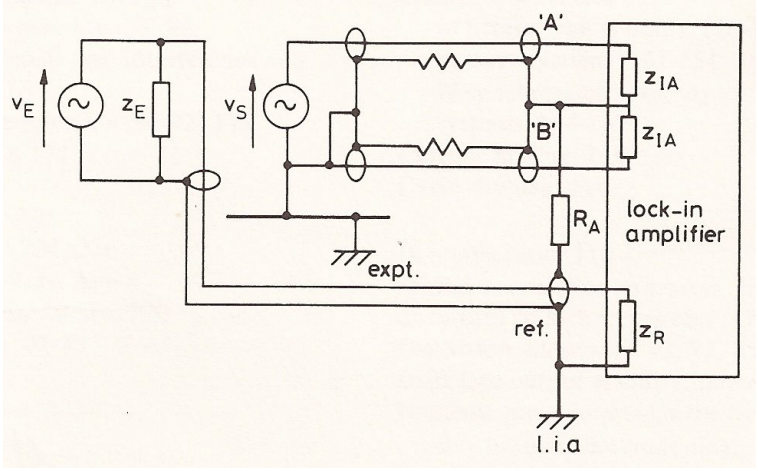

Fig A6.7 Improved experimental layout

resistance of the reference circuit. However, the spurious, synchronous, voltage set up in the signal input is often troublesome in low-level applications. A floating differential input can provide the solution in most cases. This leads us to the improved arrangement illustrated in Fig. A6.7, which also shows how to overcome the effect of the drive current. Here, the drive circuit is completely isolated from the sensitive signal circuit and contact is made to the experimental chassis at a single point. It is certainly possible that this, or some equivalent, arrangement could be arrived at by trial and error. It would be far better, however, to give some preliminary thought to ground loop problems; the alternative is almost invariable an unco-ordinated attempt to achieve "on-line" solutions when a large investment has already been made in mounting equipment and fixing cable runs.

A6.5 References

1. OTT, H.W (1976): "Noise reduction techniques in electronic systems" (John Wiley, New York).
2. MORRISON, R. (1967): "Grounding and shielding techniques in instrumentation" (John Wiley, New York).
3. Technical Note 117 (1978): "Grounding and shielding in electrochemical instrumentation - Some basic considerations" (EG&G Princeton Applied Research Corp., Princeton, NJ).
4. HOROWITZ, P., and HILL, W. (1980): "The art of electronics" (Cambridge Univ. Press, Cambridge).